Solid Oxide Fuel Cell Hybrid System for Distributed Power Generation

Semi-Annual Technical Progress Report
July 2004 to December 2004

Nguyen Minh
Principal Investigator
January 2005

Performed under DOE/NETL Cooperative Agreement
DE-FC26-01NT40779

GE Hybrid Power Generation Systems
19310 Pacific Gateway Drive
Torrance, CA 90502

Disclaimer

Abstract

This report summarizes the work performed by Hybrid Power Generation Systems, LLC (HPGS) during the July through December 2004 reporting period under Cooperative Agreement DE-FC26-01NT40779 for the U. S. Department of Energy, National Energy Technology Laboratory (DOE/NETL) entitled "Solid Oxide Fuel Cell Hybrid System for Distributed Power Generation". The main objective of this project is to develop and demonstrate the feasibility of a highly efficient hybrid system integrating a planar Solid Oxide Fuel Cell (SOFC) and a gas turbine. In addition, an activity included in this program focuses on the development of an integrated coal gasification fuel cell system concept based on planar SOFC technology. Also, another activity included in this program focuses on the development of SOFC scale up strategies. This task was completed during this reporting period and is detailed in a separate final topical report.

During this reporting period several SOFC stacks built with 6.3-inch diameter cells have been tested under hybrid conditions to assess their operating characteristics and the scalability of their stack design for hybrid applications. Also, preliminary theoretical and experimental study of the cell fabrication process led to the successful and repeatable fabrication of several planar SOFC cells using the tape calendaring process. Two of these cells were successfully performance tested at ambient and pressurized conditions. Under the coal study task, the impact of two advanced technologies, Ion-Transfer Membrane and mid-temperature cleanup technology, has been evaluated and estimated to improve the overall system performance of the baseline system by 0.7% and 0.2%, respectively.

Table of Contents

List of Figures

List of Tables

Executive Summary

Effort on the Integrated Gasified Fuel Cell (IGFC) system efficiency improvement task (task 1A.5) was initiated. Using the two down-selected system concepts from the original IGFC study (task 1A.4) as a starting point, opportunities to incorporate Ion-Transfer Membrane (ITM) and mid-range clean-up technology have been investigated and evaluated to determine their impact on system performance and cost. Incorporation of these two technologies is expected to yield 0.7% and 0.2% efficiency improvement, respectively. Incorporation of ITM technology may potential lead to a plant cost reduction of as much as 11% while the mid-range clean-up technology is not expected to have a significant impact on plant cost. Several system concepts have been identified that may have the potential of achieving the 60% system efficiency target. These concepts are currently being investigated.

Effort also began on the cell scalability effort (task 2.4) to demonstrate the potential of SOFC cell scalability. A preliminary theoretical and experimental study of the cell fabrication process led to the successful and repeatable fabrication of several cells having diameters greater than 12-inches. Two large cells were performance tested at ambient and elevated pressure.

Several SOFC stacks have been tested under hybrid condition to assess their operating characteristics and the scalability of stack designs. All the stacks employed 6.3-inch diameter cells. Tests were completed on one stack having 2-cells and two stacks having 5-cells. The stack designs have been leveraged from the SECA program.

During this reporting period task 2.3, SOFC Scale-Up for Hybrid and Fuel Cell Systems Conceptual Study task was completed. The results and conclusions from this work are summarized in the final topical report for this task (21).

Experimental

All experimental work currently performed on the program is conducted under Tasks 2.4 and 2.5. The test procedures and the test methods used to perform the experimental work for these tasks have been described in previous semiannual reports and in Section 2 and 3.

Results and Discussion

1 TASK 1A.5 – IGFC SYSTEM EFFICIENCY IMPROVEMENT STUDY

1.1 Scope and Objective

In 2003 the performance and economics of power generation systems based on SOFC technology and fueled by gasified coal were analyzed as part of task 1A.4. Two alternative system configurations were selected in the task that integrated a coal gasifier

with an SOFC, a gas turbine, and a steam turbine. Such systems are referred to as Integrated Gasified Fuel Cell (IGFC) systems. The two down-selected systems were projected to have system efficiency of approximately 53% on an HHV basis or approximately 10 percentage points higher than that of state-of-the-art Integrated Gasification Combined Cycle (IGCC) systems. While the study showed great promise for coal-based fuel cell hybrid systems, it assumed currently available gasifier, gas turbine, and balance-of-plant technology. There are potentially substantial system efficiency gains that can be realized if advanced technologies, currently in the conceptual phase or under development, are employed.

Under the current subtask, the IGFC system design as had been created in the original study is to be used as a starting point to evaluate the potential areas for system efficiency improvements with the objective of achieving a feasible system with a 60% system efficiency (AC power/Coal HHV) including carbon dioxide isolation. In addition, two specific tasks included in this study are to identify opportunities to incorporate Ion-Transfer Membrane (ITM) and mid-range gas clean-up technology in the IGFC system design and evaluate their impact on system efficiency and cost.

1.2 Original IGFC Study

In the original IGFC study (1) the initial cost of both selected configurations was found to be comparable with the IGCC system costs, at approximately $1700/kW. An absorption-based CO_2 isolation scheme was developed, and its penalty on the system performance and cost was estimated to be approximately 2.7% and $370/kW. In addition, an alternative CO_2 isolation scheme was developed that used pure oxygen to burn an anode exhaust stream; the burned exhaust gases, containing primarily CO_2, H_2O and N_2, is cooled to condense H_2O with subsequent isolation of CO_2. The results of this study were also reviewed at DOE (2).

For this study, the term “carbon dioxide isolation” refers to the separation of carbon dioxide from the exhaust stream without the need to pressurize the carbon dioxide stream. While it is recognized that to sequester CO_2 a high pipeline pressure may be required, the energy required to pressurize this stream was not factored into the study.

The concepts developed in the study were modeled to determine the effect of integrating an SOFC into a coal gasification power plant. As such, the system is considered to include the following islands:

- Coal Gasification, Cleanup and Air Separation Unit (ASU)
- SOFC and Gas Turbine
- Heat Recovery Steam Generator (HRSG) /Steam Turbine
- CO_2 isolation

Three concepts from the study are of particular interest:

Concept A: (without CO_2 Isolation): The gasification and ASU unit performance data were taken from an EPRI report (3). The gasification unit is based on a British Gas Lurgi (BGL) unit and the ASU includes a separate, conventional cryogenic plant. The cleanup of the synthesis gas is based on Lurgi's low-temperature Purisol process. The acid gas is sent to a conventional Claus plant with tail gas recycled to the Purisol unit. The BGL unit includes a bitumen feed to bind coal fines in addition to tar and gas liquor treatment. All of the technology adopted in the gasification and ASU island is considered available technology if a commercial plant were to be built today.

The SOFC/Gas Turbine island includes the use of multiple, pressurized SOFC modules. Each module contains separate SOFC stages. The gas compressors and gas turbines are considered state-of-the-art; while a specific unit is not available, it could be designed with performances achieved as modeled.

The Heat Recovery Steam Generator/Steam Turbine (HRSG/ST) island was modeled using a simple relationship between the available enthalpy of the hot exhaust gases from the gas turbine. A multi-pressure steam system is required to provide the necessary steam levels to the gasification/cleanup processes; while a detailed modeling of the steam levels/turbines/extractions, etc. was not performed in this study, the overall efficiency conversion of hot-gas to the HRSG to steam-cycle AC-power is judged achievable with existing technology.

Concept B: (having CO_2 Isolation): This system uses the same basic process configuration as described above with the addition of a Selexol process to remove CO_2 from the syngas.

Concept C: (having CO_2 Isolation): This system also uses a very similar process configuration as described above except for the CO_2 isolation. A feature of the planar SOFC technology is the separation of anode and cathode exit streams. By burning the anode exit streams with a pure O_2 stream from the ASU the CO_2 remains separated from the bulk of the process air. Hence, it is kept separate and expanded in a separate turbine from the cathode exhaust. After heat recovery in the HRSG, the CO_2 rich stream is cooled to condense water.

A summary of the efficiency projections from the original IGFC study, as reported in 2004, is plotted as a function of operating pressure in Figure 1. As shown, the system efficiency is 53.5% without CO_2 isolation. With CO_2 isolation, the efficiency is reduced by 2.2% to 51.3%. The cases shown as "alternate" included the use of internal heat exchangers to the SOFC module; while showing slightly higher efficiency, it was judged less preferable as it added more technical risk (high temperature heat exchangers) and would be more costly.

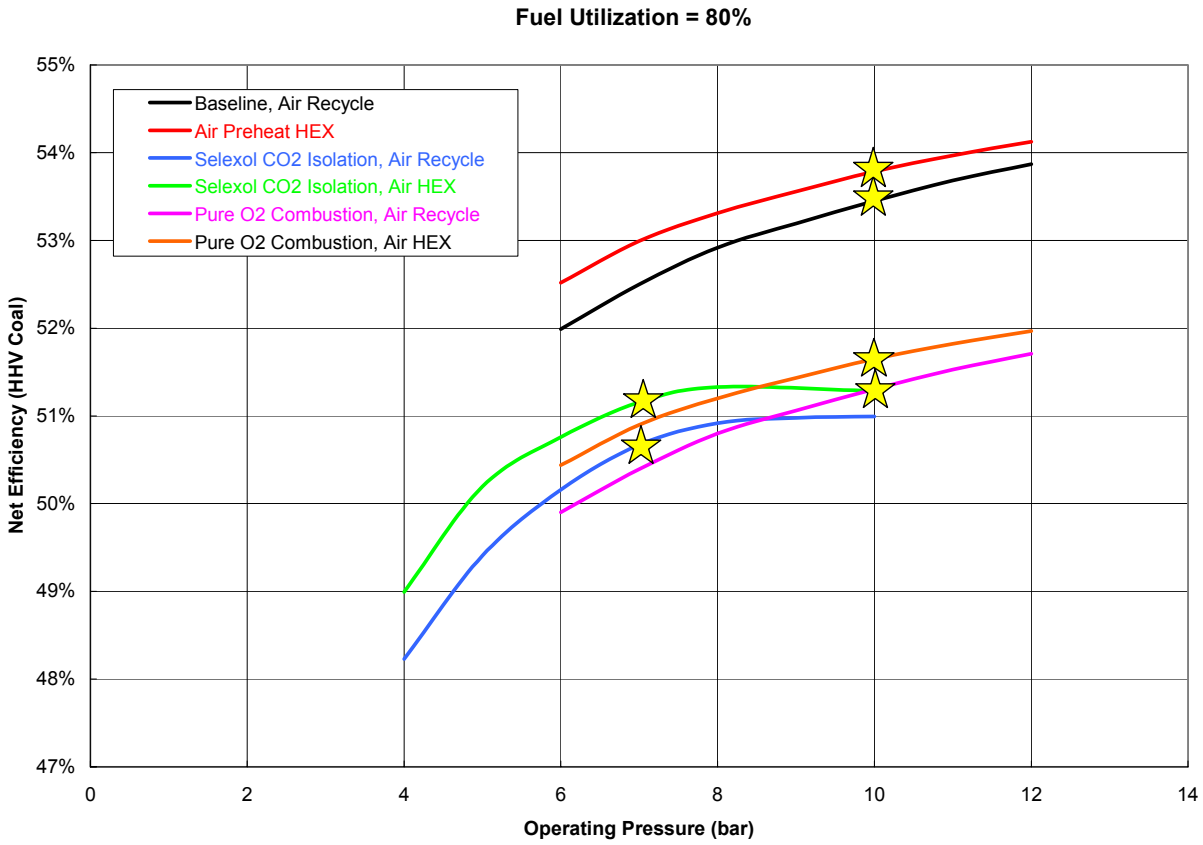

Figure 1 Summary of system efficiency projects from original IGFC study (1)

For the three cases described above, a summary and comparison of the separate power generation and parasitic contributions is provided in Table 1.

Table 1 Power Generation and Parasitic Summaries (Jan 2004 Report)

IGFC Configuration in Jan 2004 Report		Cathode Recyle	Cathode Recyle, CO2 Isolation via Selexol	Cathode Recyle, CO2 Isolation via Pure-O2 Anode Ex Combustion
POWER ISLAND SUMMARIES				
GASIFIER /AIR SEPARATION UNIT ISLAND				
Coal + Bitumen feed (HHV)	kW	541,606	541,606	541,606
Net Steam Energy from HRSG/ST Island (Note 1)	MW	95	95	95
Clean Syngas to SOFC/GT Island (LHV)	kW	433,396	433,396	433,396
Clean Syngas to SOFC/GT Island (HHV)	kW	487,548	487,548	487,548
Syngas Generation Efficiency (LHV/HHV)	%	80%	80%	80%
Syngas Generation Efficiency (HHV/HHV)	%	90%	90%	90%
Gasification & Clean-up	kW	3,196	3,196	3,196
Air Separation	kW	14,996	14,996	23,225
Sub-total Gasifier/ASU Island Power Use	kW	18,192	18,192	26,421
SOFC/GT ISLAND				
SOFC				
SOFC dc Power	kW	188581	236110	188581
Inverter loss	kW	7543	9444	7543
SOFC AC Power	kW	181038	226666	181038
Syngas Expander	kW	10162	18959	10162
Cathode Hot Air Recyle Compressor	kW	1554	2558	1554
Net SOFC	MW	190	243	190
Gas Turbines				
Combusted Gas Turbine	kW	161149	105967	68419
Cathode Exhaust Turbine	kW	0	0	98520
Air Compressor	kW	65090	63268	74733
Auxiliary	kW	0	0	0
Net Gas Turbine	MW	96	43	92
Sub-total SOFC/GT Island	MW	286	286	282
HRSG/ STEAM TURBINE ISLAND				
Steam Turbines	kW	25518	13320	26067
Net Steam Energy to Gas/ASU island (Note 1)	MW	95	95	95
Auxiliary	kW	3504	3245	3559
Sub-total HRSG/Steam Turbine	MW	22014	10075	22508
CO2 ISOLATION				
Selexol Plant	kW		2558.00	
Condensers	kW		299.00	228.00
Sub-Total:	kW		2857.00	228.00
PLANT POWER SUMMARY				
TOTAL POWER GENERATED	MW	313	302	309
POWER CONSUMED	MW	23	27	32
NET POWER TO GRID	MW	290	275	278
NET EFFICIENCY, HHV		**53.5%**	**50.7%**	**51.3%**

NOTES
1. Senesible enthalpy 77F basis, no H2O condensed

1.3 Baseline System for IGFC Extension Study

From the cases described above, Concept C was chosen as the baseline (BL) system against which to compare other systems in the current task because it include carbon dioxide isolation, over 90% isolation is possible, and an increase in its system pressure

would result in the improvement of system performance, in comparison to that of concept B.

1.3.1 Baseline-1 (BL-1) Concept Description

For the Baseline-1 System (BL-1), the exact same system configuration as concept C is used. However, two operational parameters were modified as follows:

- The SOFC operational pressure was increased from 10 bars to 12 bars. As noted above, and shown in Figure 1, an increase in pressure results in an increase in system efficiency.
- The number of stages in the SOFC module was reduced.

For the analysis of this system, the gasification and ASU unit performance data were taken from an EPRI report (3). The island consumes coal, bitumen, and limestone to produce a synthesis gas (syngas) acceptable for feed to the SOFC/Gas Turbine island. Major parts of the Gasification/ASU/Cleanup island include the following:

- Coal Handling & Preparation
- Coal gasification (BGL)
- Acid Gas Removal (Purisol)
- Sulfur Recovery (Claus & Tail Gas Treatment
- Gas Liquor Treatment
- Air Separation (cryogenic, non-integrated with Gas Turbine)
- Fuel Gas Saturation
- CO Shift

The SOFC/GT island consumes the clean Syngas produced from the gasification island to produce AC power from the SOFC modules and the gas turbine generator.

Major parts of the island include

- SOFC modules
- SOFC Inverter
- Syngas expansion turbine
- Air Compressors
- Anode exhaust gas, pure oxygen combustor
- Gas turbine
- Gas turbine generator
- Heat exchangers

The HRSG/ST island recovers heat from the hot turbine exhaust gas to generate steam for the gasification/cleanup island and to produce power from steam turbines. Major parts of the island include

- Heat exchangers to recover heat from the vitiated air exhaust gases
- Heat exchangers to recover heat from the combusted anode exhaust gases
- Multi-steam level generation including several extractions for the gasification/cleanup island
- Steam turbines and generators
- Steam cycle balance-of-plant (BOP)

The CO_2 isolation island takes the anode combusted gases after being cooled in the HRSG/ST island and condenses most of the water to isolate the CO_2. Major parts of the island include

- Air-cooled Condenser, including a blower for cooling air
- Condensate collection

1.3.1.1 Performance Assumptions

Gasification/ASU/Cleanup:

The coal, coal ash, limestone, and bitumen compositions are given in the Appendix, Table 13 thru Table 16 and are taken from EPRI TR-100376 (3).

Basic performance parameters are given in Table 2; the synthesis gas produced in shifted as shown in Table 3.

Table 2 Baseline Gasification/Cleanup/ASU Performance Assumptions

Gasification/ASU/Cleanup		
Coal as received Feed	lbs/lb coal as recvd	1
Bitumen	lbs/lb coal as recvd	0.02
Limestone	lbs/lb coal as recvd	0.04
Gasification Steam	lbs/lb coal as recvd	0.35
Oxygen (pure)	lbs/lb coal as recvd	0.63
Fuel gas saturation steam	lbs/lb coal as recvd	1.05
Power Use	MW	3.2
Steam Net Thermal Energy Consumed	MW	95
Air Separation		
Total power	MW	23.2
Pure O2 to gasifier	1000 lb/hr	82.2
Pure O2 to Anode gas	1000lb/hr	47.1

Table 3 Baseline Synthesis Gas Compositions

Mole Fractions:	Saturated Synthesis Gas	Shilted Synthesis Gas
CO	0.2934	0.1173
H2	0.1521	0.3281
CH4	0.0335	0.0373
CnHm	0.0038	0.0000
H2S+COS	<40 ppmw	<40 ppmw
CO2	0.0165	0.1925
H2O(v)	0.4855	0.3095
N2+Ar	0.0152	0.0152
Total Gas, mph	24141	24141
Pressure, psia	352	305
Temperature, F	572	905

1.3.1.2 System Efficiency Sensitivity Analysis

Parameters included in the analyses on the baseline system and prior study concepts are shown in Table 4. While not all were applied to the new baseline system, the effects of each parameter identified in the prior study are judged to be relevant to the baseline with the exception of the fuel recycle for the concept that used selexol technology for CO_2 isolation. The parameters are further described below.

Table 4 Parameters Included in Sensitivity Analyses on Baseline and Prior Study Concepts

BASELINE & PRIOR STUDY CONCEPTS	GASIFIER	SOFC						CO2 ISOLATION
	Increas in CH4 Yield from Gasifier	Operating Pressure	Fuel utilization	# of stages in each module	Cell Power Density (@ constant ASR)	ASR (@ constant power density)	Fuel Leak into Cathode	% Fuel Recycle
Prior Study Concept A: IGFC Using Cathode Air Recycle, no CO2 Isolation	x	x	x	x	x	x	x	NA
Prior Study Concept B: IGFC Using Cathode Air Recycle, CO2 Isolation Using Anode Recyle with Selexol		x	x					x
BASELINE (=Prior Study Concept C: IGFC Using Cathode Air Recycle, CO2 Isolation Using Pure-O2 Anode Effluent Combustion)		x						NA

Increase in methane yield from the gasifier: Figure 2 shows the effect of methane addition to the synthesis gas to simulate a gasifier that produces a higher methane content syngas. Methane addition raises the energy content of the fuel and also provides some additional cooling of the cells as the methane is internally reformed, improving the plant efficiency. To affect a 1% increase in system efficiency, the increase in CH4 yield as a fraction of the baseline yield is 6%.

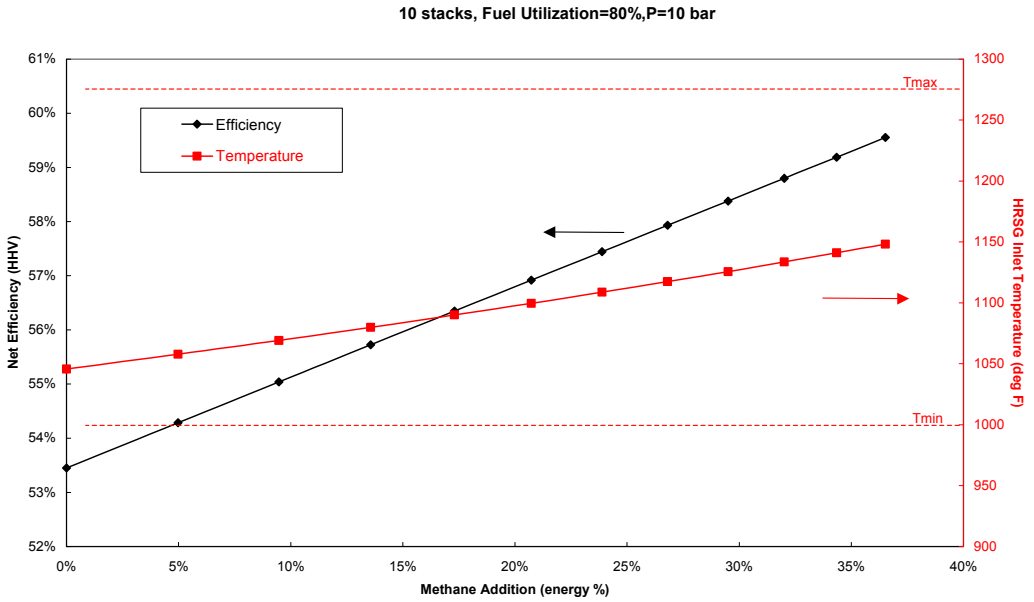

Figure 2 Baseline Sensitivity Analyses: Effect of Increased Methane Yield from Gasifier

SOFC operating pressure: The effect of pressure on the baseline is shown in Figure 1. For the baseline system, the plot indicates that increasing the pressure beyond the 12 atm would increase the system efficiency: further analyses indicated a maximum efficiency could be reached at about 18 atm. As the pressure increases, the relative power from the gas turbine increases while the power from the steam turbine decreases. This is caused by a decrease in the turbine exhaust temperature as the system pressure increases, thereby allowing less energy to be recovered by the HRSG/ST. To affect a 1% increase in system efficiency in the range from 6 to 12 atm, an increase in pressure of 4% is required. To affect a 1% increase in system efficiency in the range from 8 to 18 atm, a 7% increase in pressure is required.

SOFC fuel utilization: The effect of fuel utilization is shown in Figure 3. As the utilization increases, the SOFC power increases linearly while the energy to the gas and steam turbines decreases. To affect a 1% increase in system efficiency in the range from 70 to 90%, a 17% increase in fuel utilization is required.

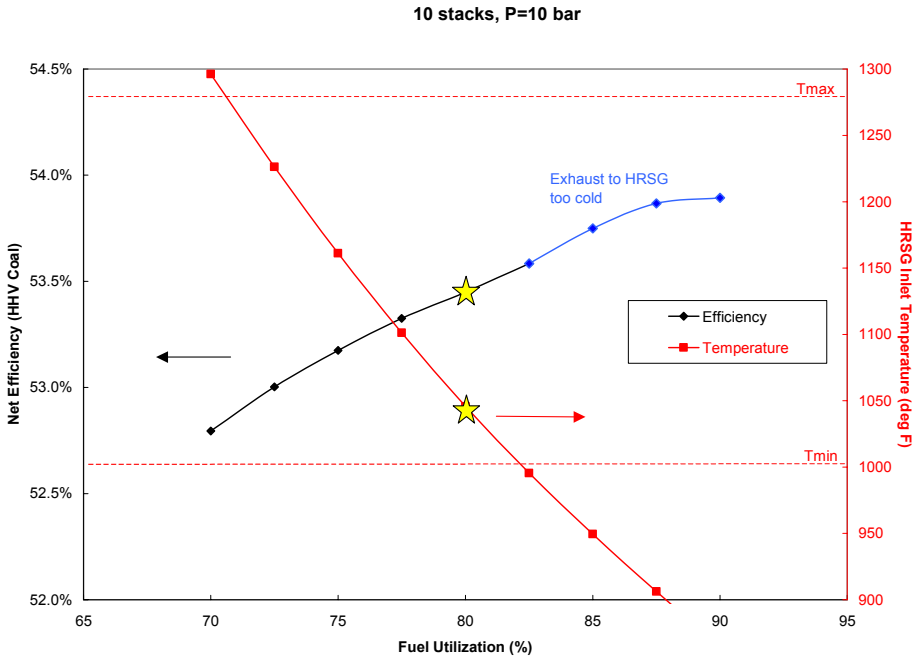

Figure 3 Baseline Sensitivity Analyses: Effect of SOFC Fuel Utilization

SOFC power density: In the prior study, an overall stack power density of 500 mw/cm^2 was assumed. Hence, if the fuel utilization, cell Area Specific Resistance (ASR) as represented in a voltage-current polarization curve of the cell, and operating conditions are kept constant, increasing the power density beyond 500 mW/cm2 result in a lower cell voltage which decreases the system efficiency.

SOFC voltage: The effect of SOFC voltage is shown in Figure 4. As with fuel utilization, increasing the cell voltage increases the amount of energy taken from the fuel cell while decreasing the energy available to the gas and steam turbines. However, increasing cell voltage also decreases the amount of cooling air required to the SOFC. To affect a 1% increase in system efficiency in the range from 0.7 to 0.77 volts, an increase of 0.04 volts is required.

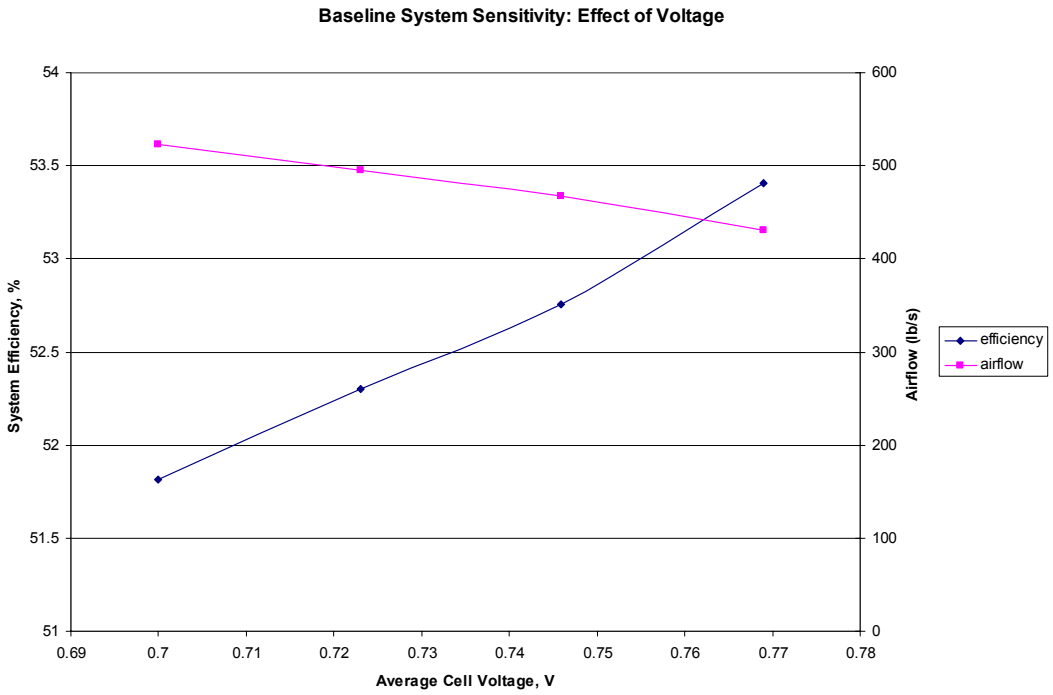

Figure 4 Baseline Sensitivity Analyses: Effect of SOFC Voltage

SOFC Area Specific Resistance (ASR): The effect of the fuel cell performance expressed as ASR is shown in Figure 5; this analysis is similar to changing the cell voltage as a power density of 0.49 w/cm^2 was maintained in the analysis. To affect a 1% increase in system efficiency in the range from 0.2 to 0.1 ASR, a decrease of 0.07 ASR is required.

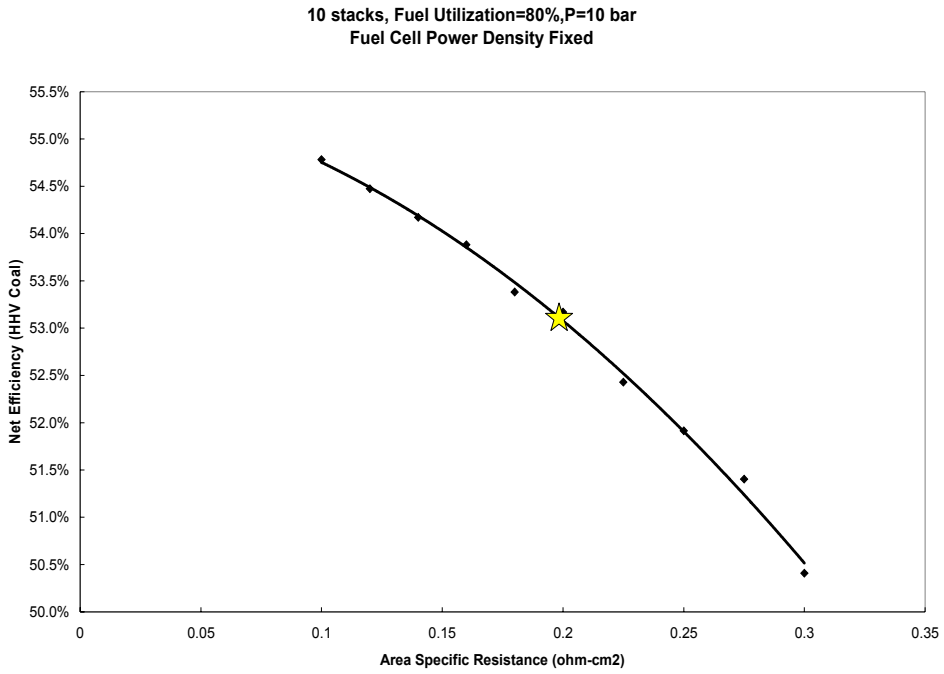

Figure 5 Baseline Sensitivity Analyses: Effect of SOFC ASR

SOFC anode fuel leak into cathode: The effect of leaking anode gas in the fuel cell performance is shown in Figure 6. The anode is maintained at a slightly higher pressure than the cathode flow in the SOFC so as to ensure any leakage would occur from the anode into the cathode chamber. Such a leak not only causes a loss of fuel utilized in the SOFC, but also affects the cathode temperature as it is assumed to combust entirely. Hence, the cooling effect of the air in the SOFC is negatively affected. To affect a 1% increase in system efficiency in the range from 0.2 to 0.1 ASR, a decrease of 0.033 % leakage is required.

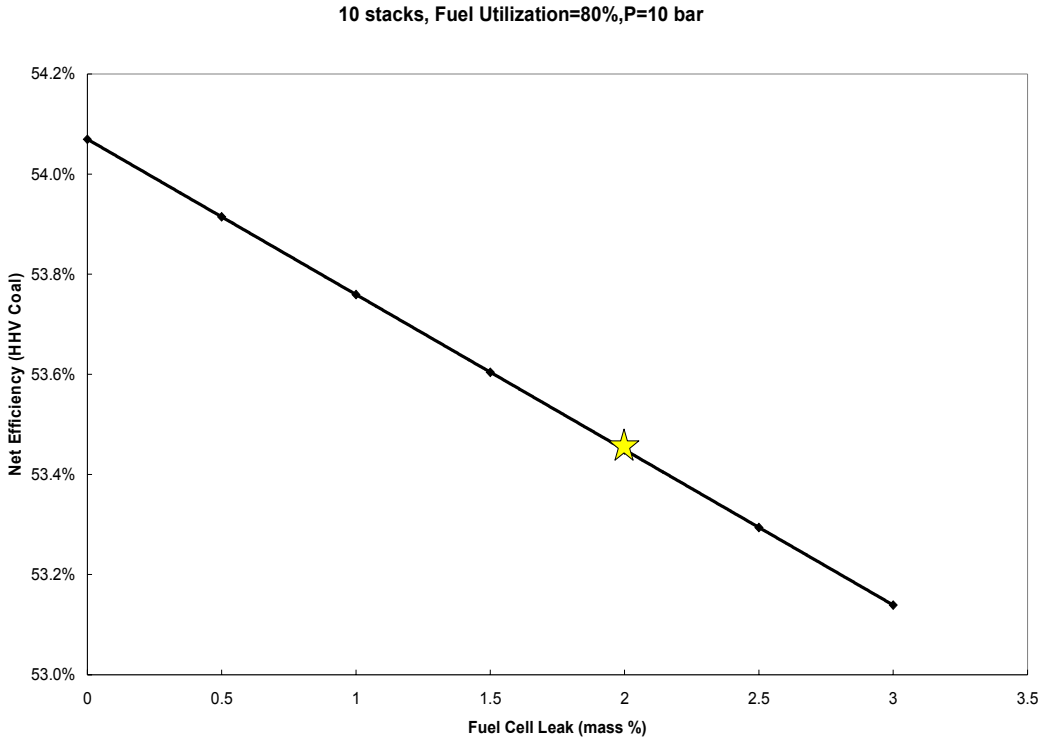

Figure 6 Baseline Sensitivity Analyses: Effect of SOFC Anode Leakage into Cathode

1.4 Study Subtasks

Specific subtasks to be completed in the current study include:

- Impact of Ion-Transfer Membrane (ITM) on the System Efficiency and Cost: Opportunities to incorporate an ITM into the IGFC system design are to be identified, including options in the gasifier, the fuel cell and the gas turbine subsystems. System analyses are to be performed to quantify effects of introducing an ITM into the baseline IGFC on the system efficiency and cost.
- Impact of Mid-Range Gas Cleanup on the System Efficiency and Cost: Opportunities to incorporate a mid-range gas cleanup subsystem into the IGFC system design are to be identified. The effects on the system efficiency and cost are to be estimated.
- Analyses of System Efficiency Improvement Opportunities: Brainstorming is to be performed to identify ideas to improve the system efficiency. Both cycle-level and component level opportunities shall be included. Analyses to quantify these improvements shall be conducted. Recommendations for any necessary future technology improvement efforts shall be made. In addition, impacts on the system cost shall be analyzed.

- Impact of Carbon Dioxide Separation: As the systems to be identified will include CO_2 isolation, the impact of the CO_2 separation on the system efficiency on the down-selected systems will be evaluated.

1.4.1 Impact of Ion Transport Membrane (ITM) on System Efficiency and Cost

ITM performance and costs estimates are based on public literature and telephone conversations with the developer, Air Products (4-9).

1.4.1.1 ITM Technology Characteristics

Technology Description: ITM technology is based on ceramic oxide materials that lose oxygen from their crystal structure at temperatures of 700°C and above, and where the loss of oxygen creates holes or vacancies in the crystal lattice. Under an applied partial pressure oxygen gradient, oxygen ions move from vacancy to vacancy within the lattice. Electrons move counter to the oxygen ions to maintain the charge balance in the material, displaying the so-called "mixed conductor" effect, as shown in Figure 7. Figure 8 shows how the devices could be stacked in a planar supported membrane device that includes laminated planar supported membrane wafers, spacer rings between each wafer, and an oxygen withdrawal tube(4-7).

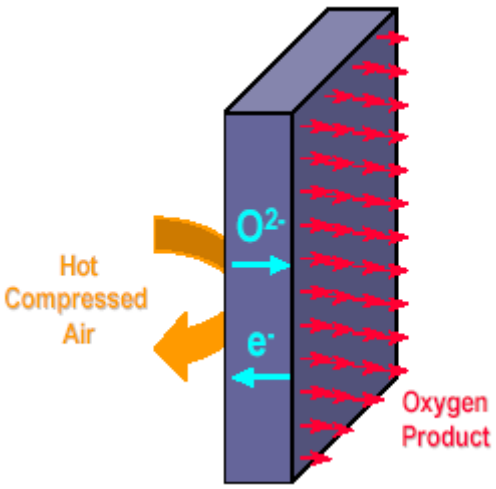

Figure 7 ITM Mixed Conductor Effect

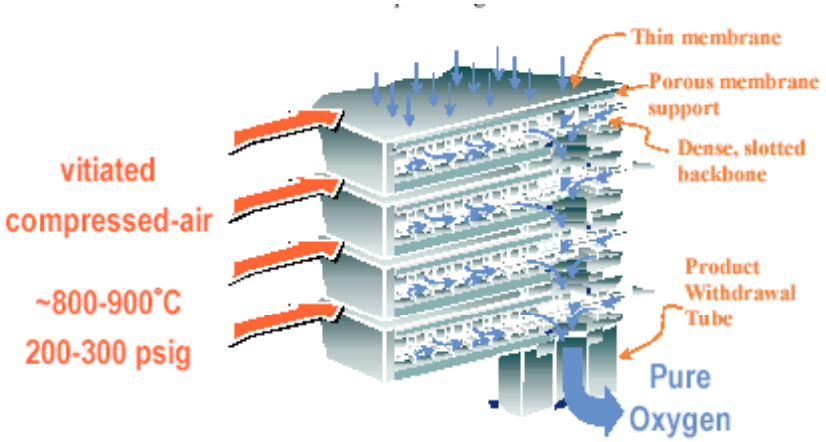

Figure 8 ITM Planar-Supported Membrane Stacking Principle

The performance of the ITM is described by the following set of equations (8):

$$R = \frac{F_{perm}}{X_{feed} F} \qquad (1)$$

$$R_T = 1 - \frac{\left(1 - X_{feed}\right)}{X_{feed}} \frac{P_{perm}}{\left(P - P_{perm}\right)} \qquad (2)$$

$$P X_{feed} \cong 7 P_{perm} \quad . \qquad (3)$$

$$X_{np} = \frac{X_{feed}\left(1 - R\right)}{\left(1 - R X_{feed}\right)} \quad . \qquad (4)$$

Where

R is the O_2 recovery fraction;

X_{feed} is the mole fraction of O_2 in the feed;

F is the feed molar flow rate;

P is the total pressure of the feed;

P_{perm} is the pressure of O_2 permeate; and

R_T is the maximum theoretical recovery.

The fraction of theoretical recovery recommended is 0.75. The device operates isothermally with a large pressure differential between the inlet feed and permeate but a small pressure difference from the air feed to the vitiated air stream. A sample calculation using the above equations and recommendations is provided in Table 5.

Table 5 Example Calculation of ITM Oxygen Recovery

SAMPLE CALCULATION OF ITM OXYGEN RECOVERY		
Required O2	- lbmol/h	3952
Feed to ITM Conditions		
Xf, Mole fraction O2	- mole fraction	0.141
P, Total Feed Pressure	- psia	172
Pperm [=P*Xfee/7] (recommended)	- psia	3.5
Rt theoretical recovery [=1-(1-Xf)/Xf*(Pperm/(P-Pperm)]	- fraction	0.875
frRt, fraction of theoretical recommended	- fraction	0.800
Actual O2 recovery fraction [=Rt*frRt	- fraction	0.700
Total Air Feed flow Required to ITM	- lbmol/h	40139

Testing: Small scale testing in 2000-2001 by Air Products included experiments conducted at the appropriate driving force for oxygen flux at approximately the commercial operating conditions of 800 to 900°C, 200 to 300 psig feed gas pressure, and typically <1 atmosphere oxygen withdrawal pressure. In addition, a 0.1 tons O_2 per day technology development unit has been operated.

Costs: The ITM has been under development by Air Products for the Department of Energy with a cost goal described as follows:

"To commercialize a tonnage-quantity ITM oxygen production process at one-third lower cost compared to competing, conventional technologies."

Several references, such as those given above, provide a cost comparison of a cryogenic vis-à-vis ITM in a coal Integrated Gasification Combined Cycle (IGCC) power plant. The costs are given at the unit level. In other words, individual component costs are not provided. For example, the costs are given on an oxygen short-Ton Per Day (TPD) basis as follows:

	$/s TPD
• ITM ASU	$13,000
• Cryogenic ASU	$20,132

1.4.1.2 ITM IGFC Concept Configurations

Four system configurations incorporating the ITM technology were reviewed. Configurations A1 and A2 are similar in that compressed air from the gas turbine air compressor is fed to the ITM directly after being preheated. The vitiated air from the ITM is fed to the cathode side of the SOFC. However, it is substantially reduced in oxygen, thereby resulting in either a low SOFC voltage or an increase in air to the system to compensate for the lower oxygen partial pressure. In A1, a permeate oxygen stream is sent to the anode exhaust burner, similar to the baseline system described above. In A2, permeate for both the anode gas burner and the gasifier are supplied. As the permeate is at low pressure, it must be compressed for the anode gas by a three-stage,

inter-cooled compressor since the combustor operates at about 11 atm. For the gasifier oxygen, an additional compressor stage is required as it operates at about 27 atm.

Configurations B1 and B2 are similar in that hot, vitiated cathode exhaust air acts as the feed to the ITM. As in A1 and A2, oxygen needs to be compressed for the anode gas burner (3-stages) and the gasifier (an additional stage).

Analyses indicate both configurations A1 and A2 would be less efficient than configurations B1 and B2, primarily due to the need for increased air flow.

1.4.1.3 ITM Impact on System Efficiency

Configurations B1 and B2 were further analyzed. For configuration B1 the ITM utilizes the cathode exit air stream to create a pure oxygen stream for the anode gas combustor. For this case, the amount of air required for the ITM to supply the anode O_2 is in excess. Hence, some air is by-passed around the ITM. The ITM permeate, at less than 4 psia, must be compressed in a 3-stage inter-cooled compressor to 173 psia.

For Configuration B2, the ITM utilizes the cathode exhaust air to create oxygen for the anode gas combustor and the combustor. The amount of air required to the ITM to supply the anode O_2 is still in excess; hence, air is by-passed around the ITM. As in Case B1, the ITM permeate must be compressed in a 3-stage, inter-cooled compressor to 173 psia for the anode gas combustor. For the gasifier, the oxygen must be additionally pressured to 465 psia by a single-stage compressor.

A comparison of the BL configuration, which uses a conventional cryogenic ASU, to Configurations B1 and B2 is given in Table 6. Each case uses the same coal feed. Configuration B2 shows a 0.7% advantage over the BL (53.5 % verses 52.8%). The efficiency improvement is due to the reduction in parasitic power associated with the ASU vis-à-vis the ITM: the net parasitic power for oxygen generation is reduced from 23 MW to 8 MW. Some similarities and differences in power required and/or generated between the systems are noted as follows:

- The coal feed for all three system concepts are identical. However, the syngas from the ITM cases is slightly more concentrated in fuel constituents as the oxygen from the ITM is purer (99.7v%) than the oxygen from a cryogenic (95v%) oxygen plant
- The power consumed in the ASU for the baseline case is 23 MW verses 8 MW for the ITM case. This represents a 65% efficiency reduction. It should be noted that the original cryogenic ASU baseline configuration is a “non-integrated” configuration (13). If the ITM were to be compared to an “integrated” configuration, where the air to the cryogenic plant is supplied using a bleed air stream from the gas turbine as air intake, the reduction in power attribute to the ITM compared to the cryogenic plant, could be less.
- The power attributed to the ITM is for compression of the permeate oxygen (at 3.5 psia) to the required pressure for gasification and anode gas burning.

- Power generated from the SOFC and expansion turbine are the same for all three cases. Likewise, power consumed from the inverter and recycle compressor are the same as the generated and consumed for all three cases
- Air flow for all three cases is the same. Therefore, the air compressor power is the same. Likewise, the un-utilized fuel from the SOFC is the same for all three cases, resulting in the same power from the combustion gas turbine. However, the vitiated air flow from the ITM is lower than the baseline, resulting in lower cathode exhaust turbine power.

Table 6 Power Generation and Parasitic Summary Comparisons: Baseline-1 & ITM Cases

SYSTEM / ISLAND		BASELINE-1 (BL-1)	ITM Case B1	ITM Case B2
GASIFIER /AIR SEPARATION UNIT ISLAND				
Coal + Bitumen feed (HHV)	MW	542	542	542
Clean Syngas to SOFC/GT Island (LHV)	MW	433	433	433
Clean Syngas to SOFC/GT Island (HHV)	MW	488	488	488
Syngas Generation Efficiency (LHV/HHV)	%	80%	80%	80%
Syngas Generation Efficiency (HHV/HHV)	%	90%	90%	90%
Gasification & Clean-up auxiliary	MW	3	3	3
Air Separation	MW	23	15	-
ITM	MW	-	3	8
Sub-total Gasifier/ASU Island Power Use	MW	26	21	12
SOFC/GT Island				
SOFC				
SOFC dc Power	MW	192	192	192
Inverter loss	MW	8	8	8
SOFC AC Power	MW	184	184	184
Syngas Expander	MW	7	7	7
Cathode Hot Air Recyle Compressor	MW	2	2	2
Net SOFC	MW	190	190	190
Gas Turbines				
Combusted Gas Turbine	MW	73	73	73
Cathode Exhaust Turbine	MW	107	104	98
Air Compressor	MW	82	82	82
Auxiliary	MW	0	0	0
Net Gas Turbine	MW	99	95	89
Sub-total SOFC/GT Island	MW	289	285	279
HRSG/ Steam Turbine Island				
Steam Turbines	MW	29	28	26
Auxiliary, ST island	MW	5	5	3
Sub-total HRSG/Steam Turbine	MW	24	23	23
CO2 ISOLATION				
Condensers	MW	0.3	0.3	0.3
Sub-Total CO2 ISOLATION	MW	0.3	0.3	0.3
TOTAL POWER GENERATED	MW	**319**	**315**	**307**
POWER CONSUMED	MW	34	28	17
Net Power To Grid	MW	286	287	290
System Efficiency, % of HHV Input	%	52.8	53.1	53.5

1.4.1.4 ITM Impact on Cost

The cost impact, based on a ROM-type estimate, is provided in Table 7.

Table 7 Cost Comparison with ITM

	SUMMARY MM$	NET POWER MW	COST $/kW	COST REDUCTION %
BASELINE-1	$488	285	$ 1,710	--
ITM-B1	$453	287	$ 1,578	8%
ITM-B2	$447	289	$ 1,544	11%

1.4.2 Impact of Mid-Range Gas Cleanup on System Efficiency and Cost

Mid-range gas cleanup performance and cost estimates are based on public literature, telephone conversations with the developer, RTI, and GE engineering judgment (10-16). Cost data were not available in the public literature. Other data regarding systems required to remove trace compounds such as Hg, were also not available.

1.4.2.1 Mid-Range Gas Cleanup Technology Characteristics

Technology Description: Research Triangle Institute (RTI) and Kellogg Brown and Root (KBR) are jointly developing a pressurized, mid-range temperature desulfurization process capable of desulfurizing a sour and wet syngas. The process includes KBR's patented transport reactor technology and RTI's proprietary zinc oxide based sorbent for sulfur removal from gaseous streams, called RTI-3. KBR's unit consists of two coupled transport reactors, a sulfur absorber and a sorbent regenerator, as shown in Figure 9. RTI-3 zinc oxide sorbent removes H_2S and COS from syngas by circulating it continuously in the absorber and also transferring a portion of it from the absorber to the regenerator and vice versa. The following reactions occur:

- ZnO + H2S = ZnS + H2O (absorber)
- ZnS + 3/2 O_2 = ZnO + SO_2 (regenerator)

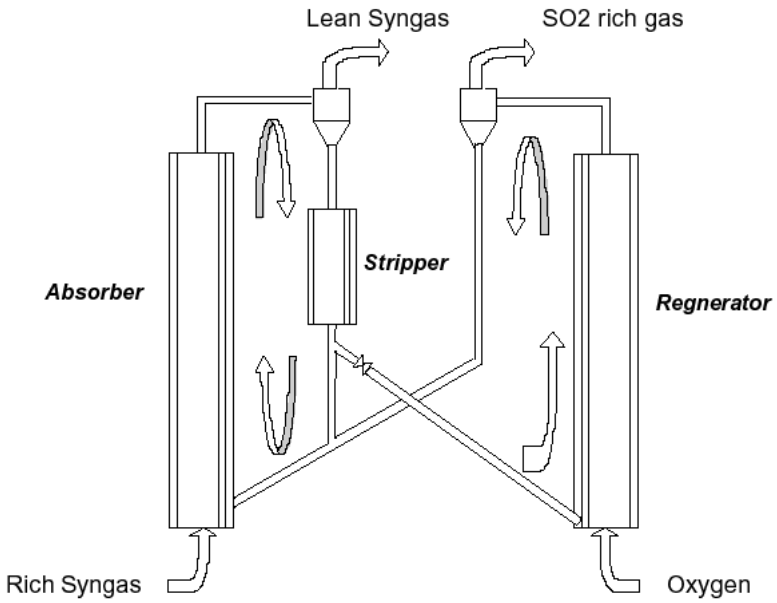

Figure 9 Warm Gas Cleanup Process

Testing: Production of RTI-3 has been done up-to 200 to 1000 lb batches by Süd-Chemie, Inc. of Louisville, KY. Using a simulated syngas stream with 60 vol% steam and 0.7% (7,000 ppmv) H2S and 0.035% (350 ppmv) COS, RTI-3 consistently reduced the effluent sulfur concentrations to non-detectable levels at 600ºF and 130 psig. Regeneration of the sorbent was successfully demonstrated at temperatures above 1000ºF with significant sulfur removal per pass. Post-test analysis of the RTI-3 confirmed earlier attrition test results with essentially no fines generation (< 20 micron) or change in the particle size distribution. In a 3 ton per day gasification unit at ChevronTexaco's Montebello Technology Center in South El Monte, CA, 17,200 scfh of warm syngas enters the absorber at 600 to 800ºF. RTI-3 is continuously regenerated in the regeneration reactor. This reaction occurs at 1230 - 1300ºF. As the reaction is highly exothermic, typically 6 to 10 volume % O_2 in N_2 is used as the oxidant gas. The oxidant enters the regenerator at about 1100ºF and from the heat generated in the regenerator reaction, the temperature increases to 1250ºF to 1300ºF. Typically, sulfate formation is avoided by only partially regenerating the sorbent. The high temperature of the returning, regenerated sorbent provides the energy needed to boost the temperature of the incoming syngas from 500 ºF to 600 – 800 ºF.

As noted in the literature sources, RTI has done a significant amount of work to prove the capabilities and reliability of their system. Of particular interest is their collaborative work with other organizations including Chevron/Texaco and KBR. In addition, there has been recognition of the necessity to develop mercury and ammonia cleanup processes, which are critical to producing an acceptable gas for a power production application. They have also developed a Direct Sulfur Recovery Process (DRSP) that

would replace the CLAUS Plant in the sulfur removal process, with a slight possible increase in efficiency of sulfur removal.

In summary, RTI has developed a sulfur removal process from syngas with the following characteristics:

Operating Temperature Ranges:

- 500^{o}F to 1200^{o}F Overall Range
- 700^{o}F to 800^{o}F Optimum Range

Demonstrated Capabilities:

- Syngas with 5% H2O content – H_2S and COS below 1 ppm
- Syngas with 20% H2O content – H_2S and COS below 1 ppm
- Syngas with 50% H2O content – H_2S and COS below 1 ppm
- Syngas with 63% H2O content – H_2S and COS at single digit ppm level

Costs: Although their system is cost competitive (~$60-$75/KW) with other sulfur removal schemes such as Amine and SELEXOL plants, the main advantage of their system is obviating the need to cool the syngas down to the 100^{o}F level necessary for traditional sulfur removal systems.

Sulfur Recovery Options and Chemistry: The process described above and utilized in this study includes the DSRP process for recovering sulfur after it is removed from the syngas. Three alternatives of many possibilities for conversion of SO_2 to a solid or liquid product from the Warm Gas Cleanup system are as follows:

1. Elemental sulfur from a Direct Sulfur Recovery Process: Figure 10 shows how the RTI regenerator off-gas (ROG) is processed in a Direct Sulfur Recovery Unit from the Regenerator Off-Gas. As shown in the sulfur chemistry given in the diagram, for each mole of sulfur, 2 moles of an equivalent hydrogen reducing gas (H_2 +CO) are required. In our baseline system, this represents over 1% of the synthesis gas produced;
2. Sulfuric acid production: Figure 11 shows the production of sulfur from the ROG. This requires no fuel gas slip stream;
3. Reduction of SO_2 with Anthracite: Figure 12 shows the ROG used a direct reduction process with anthracite (or coal) to convert the SO_2 to elemental sulfur.

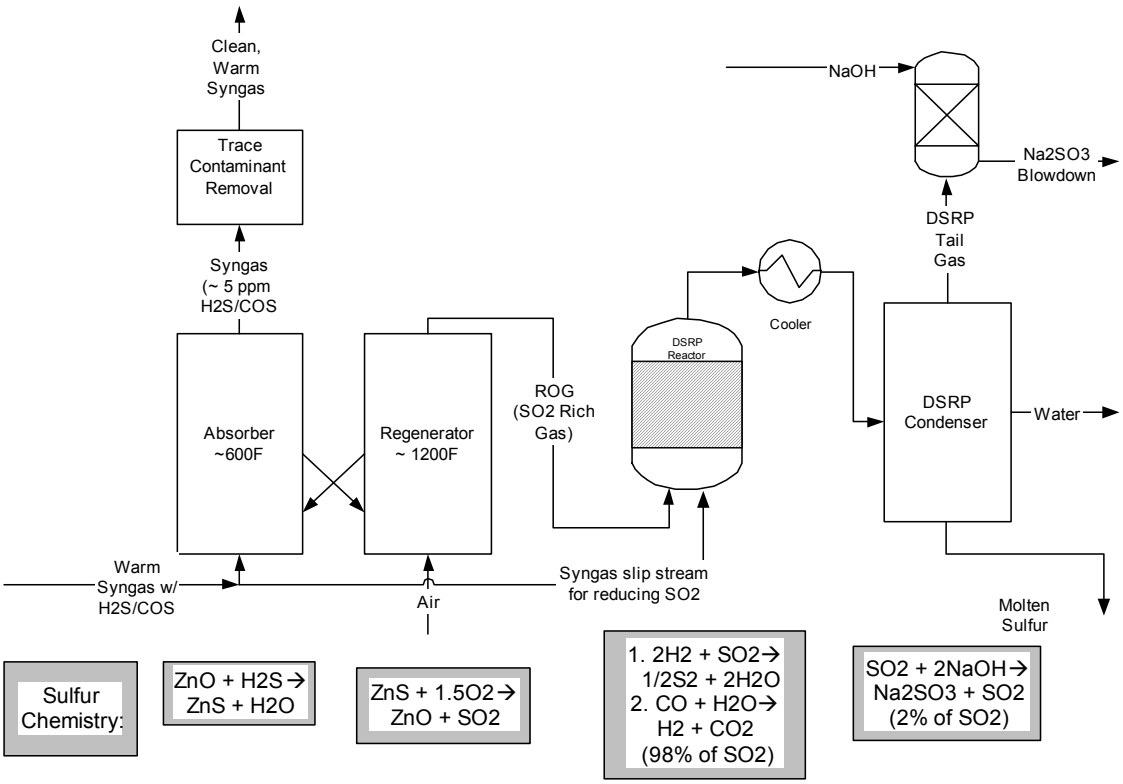

Figure 10 Warm Gas Cleanup System: Sulfur Recovered as Elemental Sulfur

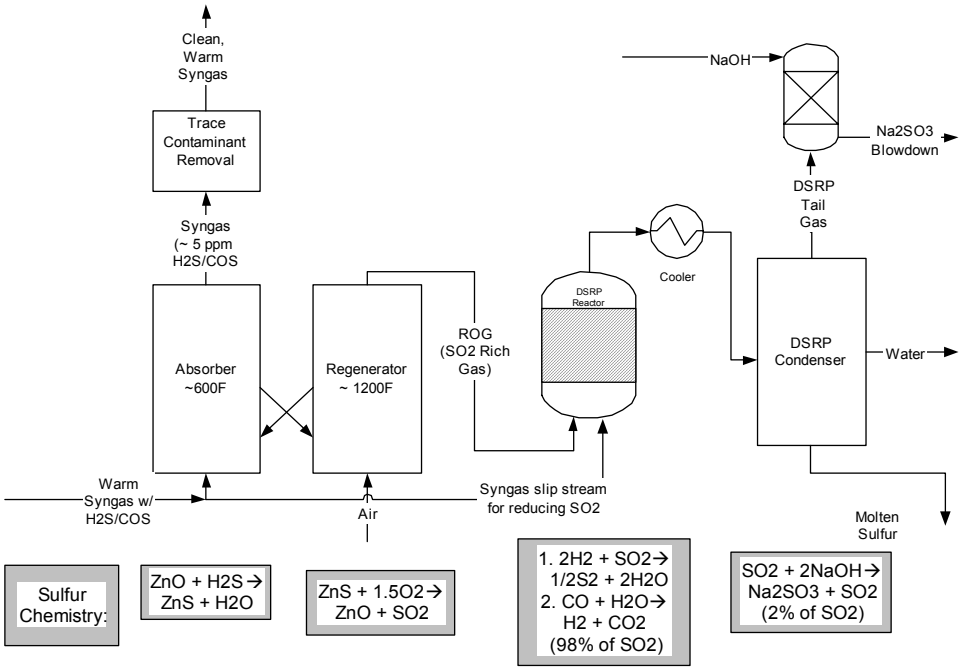

Figure 11 Warm Gas Cleanup System: Sulfur Recovered as Sulfuric Acid

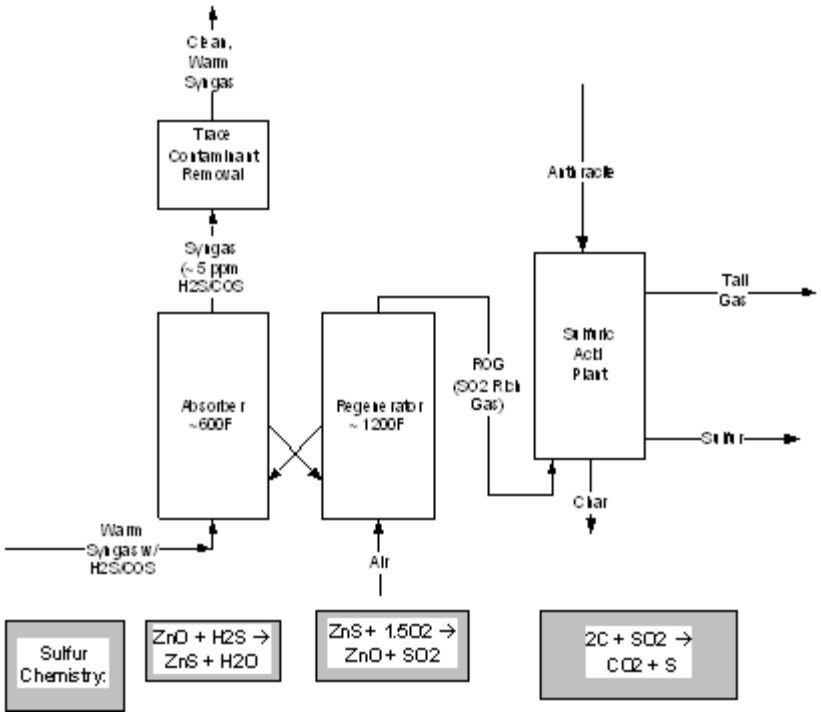

Figure 12 Warm Gas Cleanup System: Sulfur Recovered as Sulfur from Anthracite Reduction

1.4.2.2 Mid-Range Gas Cleanup Concept Configurations

Baseline Purisol Process: In the baseline system, using the BGL gasification system, raw syngas at approximately 280 ^{o}F is cooled to approximately 100 ^{o}F and sent to the Purisol process for sulfur removal from the syngas, as shown in Figure 13. The Purisol system consists of a Purisol absorption unit, which absorbs sulfur from the syngas and yields a clean syngas and an acid gas stream. This acid gas stream is sent to a Claus unit, which converts the acid gas to elemental sulfur. The Purisol unit requires steam for the reboiler, and pumping power for the solvent circulation pumps. The Claus unit requires fuel gas for oxidation of the acid gas. An additional heat load in the Purisol system is the heat load resulting from the difference of heat duties between the cool-down of the raw syngas to the Purisol operating temperature.

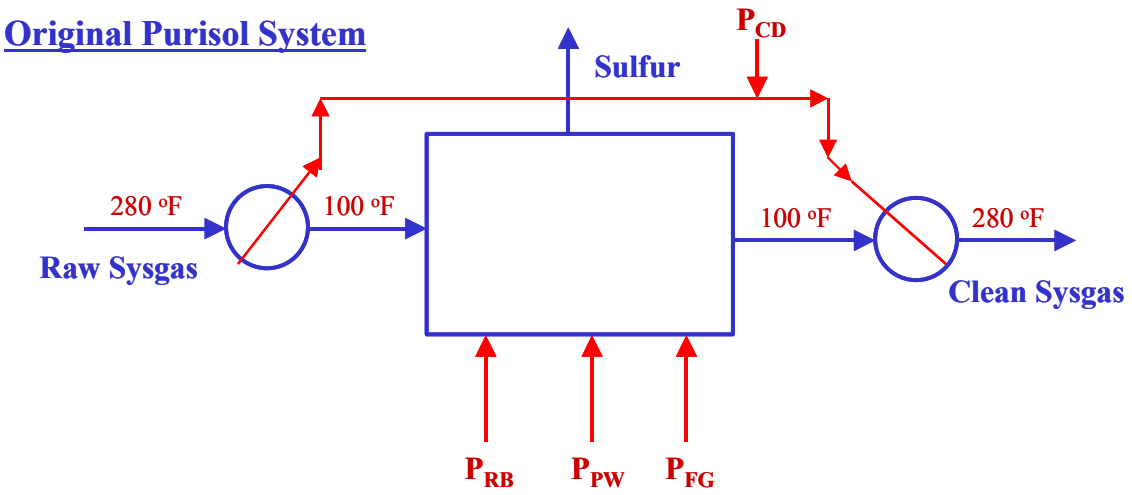

P_{CD} = Cooldown Equivalent Power = 1610 KW

P_{RB} = Reboiler Equivalent Power = 610 KW

P_{PW} = Pumping Equivalent Power = 580 KW

P_{FG} = Fuel Gas Equivalent Power = 110 KW

Total Required Power: 2900 KW

Figure 13 Low-Temperature (Purisol) Gas Cleanup Process (original) in Baseline IGFC

Mid-Range Gas Cleanup in Baseline: Substituting the RTI system into the baseline, raw syngas at approximately 600 °F is sent to the RTI system for removal of sulfur from the syngas as shown in Figure 14. The RTI system consists of a warm gas absorption unit, which absorbs sulfur from the syngas and yields a clean syngas and an acid gas stream. This acid gas stream is sent to a Claus unit, which converts the acid gas to elemental sulfur. Additional mercury and ammonia absorption units must be included in order to provide a clean syngas suitable to the requirements of the fuel cell stack. However, the processes to remove these contaminants are not well defined in the literature cited above.

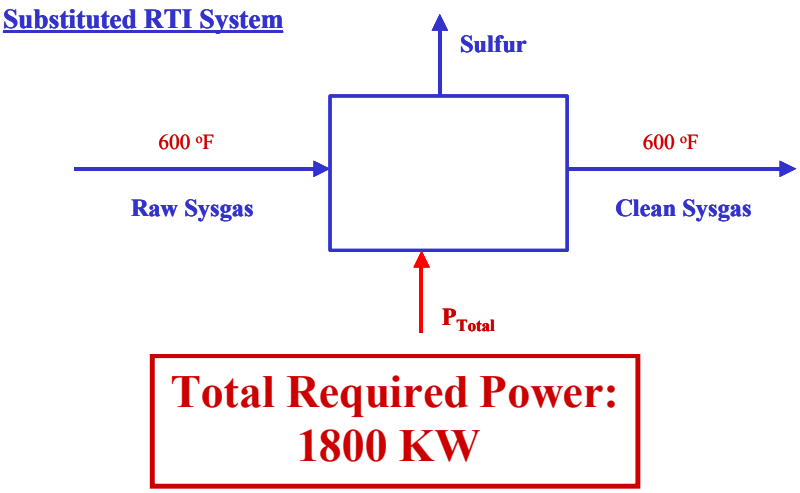

Figure 14 Mid Range Gas Cleanup Process (RTI) Inserted in Baseline IGFC

1.4.2.3 Mid-Range Gas Cleanup Impact on System Efficiency

Analysis Method: A differential analysis was performed to determine the effects of replacing the Purisol acid gas removal system, which is part of the BGL gasifier system, with an RTI warm gas sulfur removal system. All heat loads in the process systems were converted to an equivalent electrical power produced by the steam turbine. The total required power for each system was determined and the net difference is the power saving resulting from replacement of the Purisol system by the RTI system.

The resulting power requirements, and the total required power, for the Purisol system and substituted mid-range gas cleanup processes are shown in Figure 13 and Figure 14 to be 2,900 and 1,800 equivalent kilowatts of power. The net power savings estimate via this differential analysis procedure is 1,100 kW. This represents approximately a system efficiency performance improvement of only 0.2% based on a coal and bitumen feed of 541 MW.

1.4.2.4 Mid-Range Gas Cleanup Impact on Cost

There were no specific cost references in the literature cited above to indicate the costs of the mid-range gas cleanup system. However, in a telephone conversation, as noted above, costs were estimated to be in the order of $60-$75/kW of net system power produced. This is comparable with other typical gas cleanup processes. It is judged that the cost impact, assuming the performance estimated above, is within the fidelity of the ROM-type estimate.

1.4.3 Analysis of System Efficiency Improvements

As shown above, the baseline efficiency was improved to 53.5% by inserting the ITM for oxygen. Another 0.2% may be achieved by inserting a mid-range gas cleanup process. The baseline configuration with these performance improvement incorporated is still well below the 60% efficiency goal for this study. Table 8, shows the power production

and consumption for the baseline prior to the incorporation of the advanced technologies. Note that the total power generators before subtracting any of the power consumers only adds up to 56%, well below the target 60% efficiency. Hence, for this configuration to reach 60%, the efficiency of the generators would have to be improved significantly. Any improvements that the ITM would have, even if reduced to zero power for the ASU, would not result in a system efficiency of 60%. Likewise, if the power associated with gas cleanup were reduced to zero, the system would still not achieve 60% efficiency.

Table 8 BL-1 System Net Power Generators and Consumers

BASELINE-1 NET POWER GENERATORS & CONSUMERS	% of Feed HHV
Power Generators:	
SOFC AC	33.6%
Gas Turbines (Cathode Exhaust+CombGas -Air Comp)	18.3%
Syngas Expansion Turbine	1.4%
Net Steam Turbine	4.4%
Subtotal Generators	57.6%
Power Consumers:	
ASU (cryo)	4.3%
Gasifier & Clean-up	0.6%
CO2 Isolation	0.1%
Subtotal Power Consumers	4.9%
NET System	52.7%

Further analysis of the baseline power generation and consumer is illustrated in Figure 15. Since the SOFC is the largest generator, an improvement to its performance is a likely candidate to increase efficiency. This will be analyzed further below.

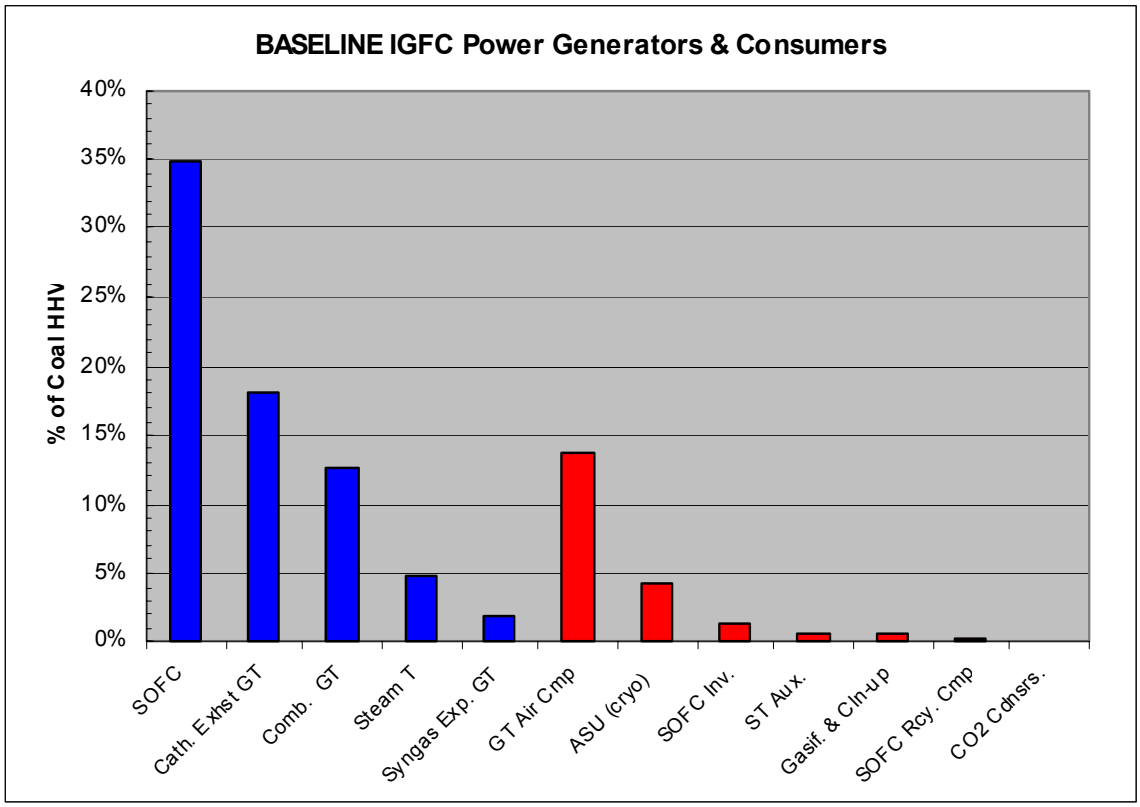

Figure 15 Baseline IGFC Power Generators and Consumer Comparisons for BL-1

1.4.3.1 Entitlement Analysis for Baseline Configuration with ITM and Mid-Range Gas Cleanup

The following "entitlement analysis" is provided as a means to estimate which selected processes may possibly be improved to affect an overall improvement in the system efficiency. "Entitlement" is a term that implies the maximum possible benefits from engineering and/or technical developments. The analysis presented here represents GE engineering and technical judgment.

BGL Gasifier Entitlement: A differential analysis was performed to determine the effects of an optimum BGL gasifier in the baseline system. In order to maximize the level of chemical energy (for conversion to power in the SOFC), the BGL gasifier output syngas was modified to contain no CO_2. The level of other constituents in the syngas was maintained at the original level. This resulted in decreased coal, limestone, oxygen and process steam requirements for the gasifier.

An energy balance for both the original BGL IGCC system, and the modified BGL IGCC system with maximum entitlement are given in Table 9.

Table 9 Gasifier Entitlement Analysis

Original BGL IGCC System

Performance Summary:

Gross Power Gen.		
- Gas Turbines	- kW	384000
- Steam Turbine	- kW	135100
Sub-Total:	- kW	519100
In-Plant Power Cons.		
- Gasification	- kW	6855
- Air Separation	- kW	32097
- Combined Cycle	- kW	3781
- Cooling Water CC	- kW	773
- Cooling Water PP	- kW	1908
- BOP+Misc	- kW	2919
Sub-Total:	- kW	48333
Net Power To Grid	**- kW**	**470767**

Heat Input, HHV	- MMBtu/h	3964.4
Net Heat Rate, HHV	- Btu/kWh	8421.2
Net Efficiency, HHV	**- %**	**40.53**

BGL IGCC System With Maximum Entitlement

Performance Summary:

Gross Power Gen.		
- Gas Turbines	- kW	383500
- Steam Turbine	- kW	119170
Sub-Total:	- kW	502670
In-Plant Power Cons.		
- Gasification	- kW	6821
- Air Separation	- kW	27926
- Combined Cycle	- kW	3525
- Cooling Water CC	- kW	721
- Cooling Water PP	- kW	1779
- BOP+Misc	- kW	2800
Sub-Total:	- kW	43570
Net Power To Grid	**- kW**	**459099.9**

Heat Input, HHV	- MMBtu/h	3788.3
Net Heat Rate, HHV	- Btu/kWh	8251.5
Net Efficiency, HHV	**- %**	**41.36**

Based on these estimates, the maximum BGL gasifier entitlement is of the order of ~ 0.8% for the IGCC system. Since it is improbable that the gasifier can operate under conditions corresponding to this maximum entitlement, it was modified by a 'realization factor' of 0.3 to yield an assigned entitlement increase of 0.3%.

Sulfur Removal Entitlement: Additional efficiency improvements for the IGFC system may be possible if CO_2 could be removed from the syngas process stream in the sulfur removal block of the gasification process island. The syngas exiting the reactor is saturated, and a sour gas shift replaces the previous shift reactor. This shift is followed by the RTI gas cleanup system for H_2S and COS sulfur removal, and 90% of the CO_2 in the syngas stream is removed by a Selexol CO_2 removal process. The resulting syngas could then be sent to the SOFC.

Energy requirements for the syngas saturation before the sour gas shirt reactor appear to be similar to saturation requirements for the original BGL gasification system. Reasonably detailed calculations for the Selexol CO_2 removal process indicate that a net equivalent power requirement of 3.6 MW would be necessary for this system. This power requirement was balanced against the added power output of the SOFC, and a resulting efficiency (HHV basis) increase of 0.3 % could be realized from the sulfur removal system for the case where 90% of the carbon dioxide was removed prior to introduction of the syngas into the SOFC.

Oxygen Plant Entitlement Results: Various schemes to modify the SOFC system do not result in any significant change in the oxygen concentration of the vitiated air entering the ITM process. Therefore, there is no significant entitlement for the oxygen plant after inserting the ITM in the baseline IGFC configuration.

Combined Cycle Entitlement (Effects of Turbine/Compressor Efficiencies): For the baseline system SOFC/GT island section, compressor efficiencies of 88% and turbine efficiencies of 91% were chosen, based on internal GE data. Other turbomachinery components are likely to be less efficient, because of their smaller size or the way they are operated. The stand-alone expanders were given an 89.3% efficiency, while the recycle blower and other motor driven blowers had a net 80% efficiency. The electrical machinery is usually highly efficient; generators and motors with 99% efficiency are not uncommon. Most of these efficiencies given are above or close to, entitlement. Low-temperature firing, low- pressure to medium-pressure turbomachinery components with a relatively small stage count are not known to achieve these levels of efficiency. Figure 16 and Figure 17 show the sensitivity of the plant efficiency to air compressor and turbine efficiencies respectively. In these plots, all the compressors and turbines in the plant are given the same efficiency, regardless of size. Heavy frame, advanced turbomachinery components are also shown. It could be seen that the sensitivity to turbomachinery components is relatively small. The total gas turbine island entitlement gain is estimated to be 0.3%, albeit at perhaps an increase in cost.

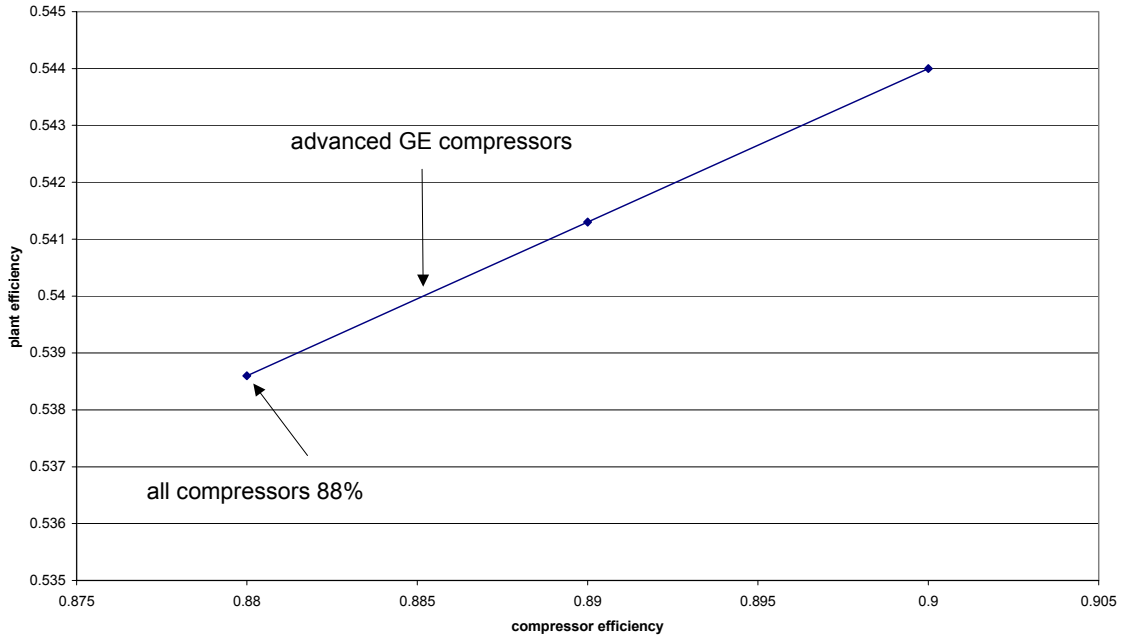

Figure 16 Entitlement Analysis: Effect of Compressor Efficiency on System Efficiency

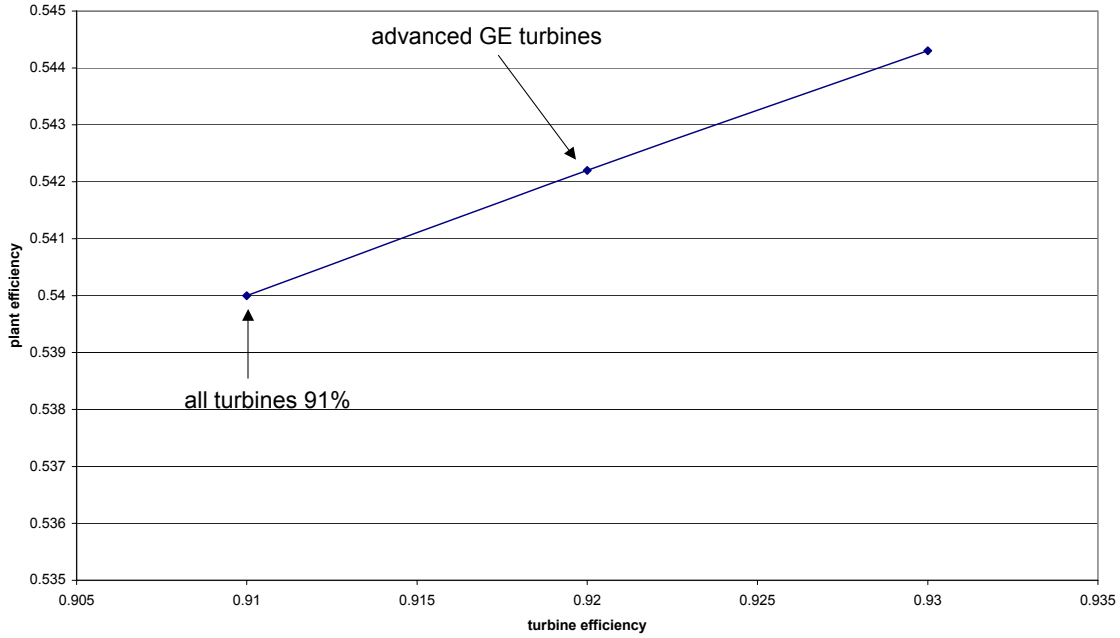

Figure 17 Entitlement Analysis: Effect of Turbine Efficiency on System Efficiency

SOFC power conversion entitlement: SOFC generators produce DC power, which must to be converted to high voltage, 3-phase AC power before it is connected to the grid. Studies done in the "SOFC Scale-up" project has shown that power conversions efficiencies of 96% are theoretically possible, by eliminating or reducing losses from filtering in the inverter components and by connecting transformers in a novel manner to multiple inverter units. With only switching losses in the inverters, and minimal ohmic losses in the transformers and conductors, this is likely the entitlement in power conditioning. The entitlement gain from SOFC inverter power is assumed to be negligible and is assumed a value of 0%.

Combined Cycle Entitlement (Effects of Fuel Cell Operating Voltage): Fuel cell operating voltage is a measure of fuel cell efficiency; hence, increasing the voltage from the nominal 0.7 V to a higher value should be helpful. However, as the operating voltage increases, other effects are observed:

(1) Since the fuel cell produces less excess heat with increasing operating voltage, the air flow in the cycle goes down as shown in Figure 18. Although the power produced from the fuel cell system goes up as shown in Figure 19, the gas turbine and steam turbine power decreases.

(2) With the baseline configuration where an ITM is inserted to provide all the oxygen requirements, restrictions can be imposed on the operating voltage. The O_2 content of the fuel cell exhaust decreases with operating voltage, e.g. as the voltage is increased from 0.694 to 0.773, the O_2 mass % goes from 13.9% to 11.2%. The ITM works with a fixed O_2 mass requirement, so as the voltage goes

up, the ITM demands more and more of the exhaust stream. At around 0.775 V, the entire exhaust stream is consumed by the ITM. This provided an upper limit of operation of the fuel cell with ITM under these assumed baseline conditions.

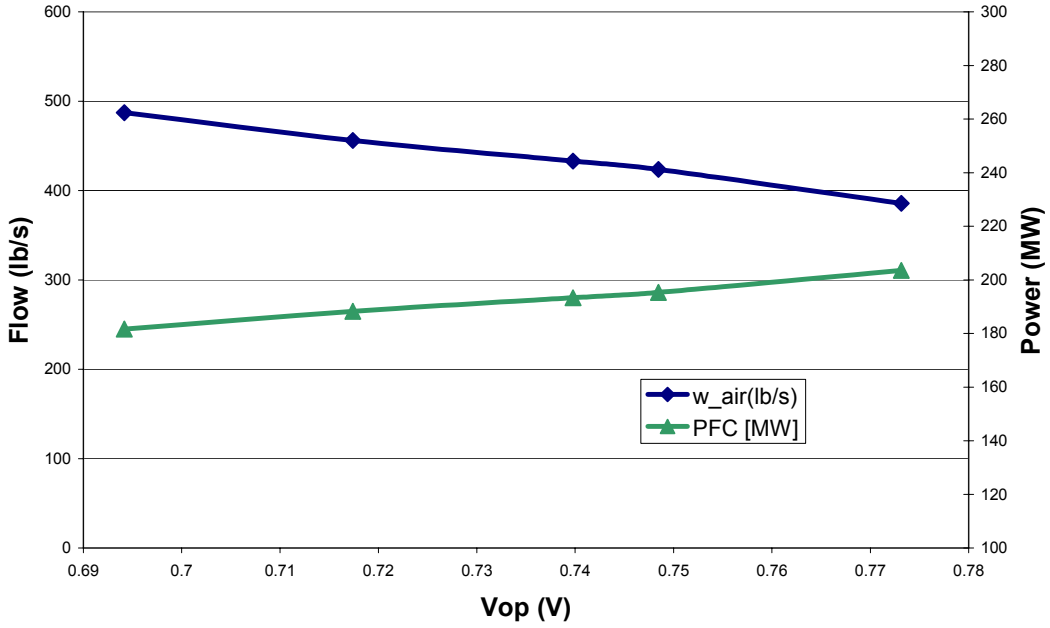

Figure 18 Entitlement Analysis: Effect of Average Cell Voltage on Air Flow to the SOFC in the Baseline System Configuration

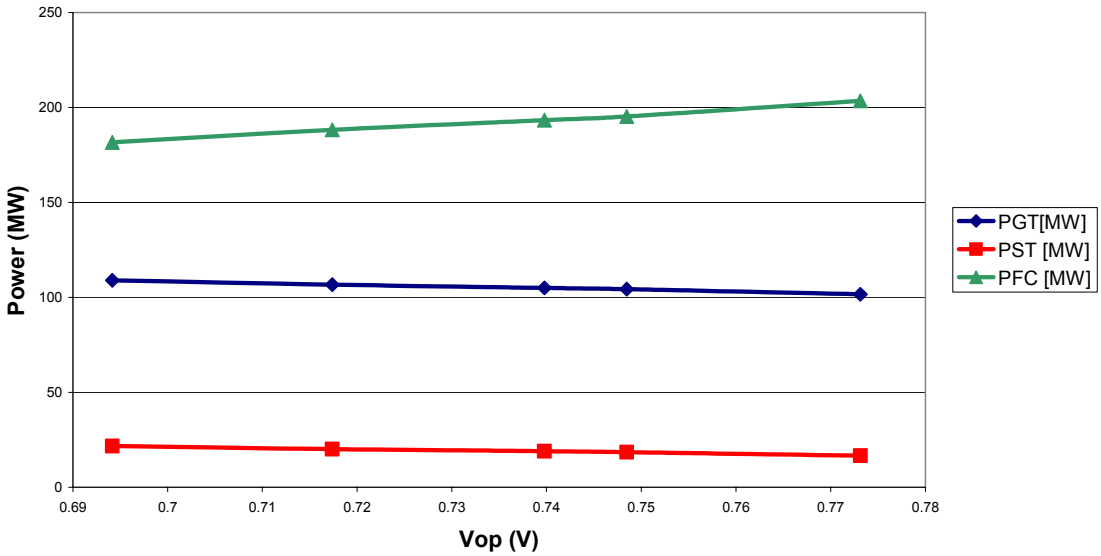

Figure 19 Entitlement Analysis: Effect of Average Cell Voltage on SOFC, GT and ST in the Baseline System Configuration

In the baseline system configuration with an ITM inserted, increasing the voltage from 0.7 to 0.77 increases the efficiency by 1.7%. Since the ITM system cannot go beyond 0.775 V, this could be considered the efficiency entitlement of increasing voltage.

Final efficiency improvement: From the above analysis, we can project possible increases in the baseline system results, as follows:

Baseline Efficiency, %		52.8
ITM technology insertion	0.7	
Mid-T Cleanup insertion	0.2	
Subtotal		0.9
Improved System Efficiency, %		53.7

In addition to Tasks 1 and 2, we have determined Upper-Limit Entitlements for the IGFC System:

Improved System Efficiency, %		53.7
Upper-Limit Process Island Entitlement	0.6	
Upper-Limit Combined Cycle Entitlement	0.3	
Upper-Limit Fuel Cell Voltage Entitlement	1.7	
Total Upper-Limit Entitlement		2.6
Final System Efficiency with Upper-Limit Entitlement		56.3

Note that the final realistic system efficiency in the year 2020 time frame is expected to be less than this Upper-Limit Final System Efficiency

1.4.3.2 Brainstorm

Brainstorm was initiated with the objective of generating ideas that would lead to systems with 60% system efficiency within the technologies' entitlement and feasibility. The problem statement for this brainstorming was as follows:

- Identify technologies which, if developed to their entitlement, can be implemented in an IGFC system and can significantly (>1%) improve the overall system efficiency
- Identify an IGFC system configuration that, if all incorporated technologies are developed to their entitlements', could be shown by analysis to result in a 60% system efficiency

The concepts that resulted from this brainstorming session, summarized below are currently under investigation.

Baseline-2 System Configuration: The basic system configuration is as shown in BL and BL-1. As noted in the entitlement analysis, a system efficiency of 56% is judged

possible. By changing the following operational parameters, the system efficiency could be improved further:

- SOFC pressure: preliminary analysis indicated system efficiency gains beyond 12 atm are possible
- SOFC operating temperature: by increasing the operating temperature of the SOFC, the temperature level of the wastre heat from the SOFC to the GT and ST cycles would increase, resulting in higher conversion of waste heat to power
- Gasifier methane yield: if the gasifier can be operated to give higher methane yields, the internal reforming capability of the SOFC could result in lower air flows. In simple cycle and gas-fueled SOFC hybrid systems, this usually results in higher system efficiencies as the cooling air to the SOFC can be reduced. However, it is not known if the adopted BGL gasifier could operate to give higher methane yields at this time.

These parameters will be investigated further.

Dartmouth College Study: Figure 20 gives a schematic taken from the Ref. 17reference. Characteristics of this concept include the following:

Gasifier:

Type:	Fluidized bed, two-stage, CO_2 Acceptor
Operating Pressure	10 Atm
Temperature	800 C (gasifier)
	1027 C (regenerator)
Gas Cleanup	S captured primarily in regenerator
	S polishing (no power used)
Air Separation	None
SOFC	
Operating Pressure	10 Atm
Cathode Air Temperature In	747 C
Cathode Air Temperature Ex	939 C
Air Temperature Rise	192 C
Oxygen utilization	~0.75
Fuel utilization	0.79
Cell voltage	0.7
Gas Turbine	

Efficiency	0.86
Steam Turbines	
High Pressure	40 atm
Low Pressure	10 atm

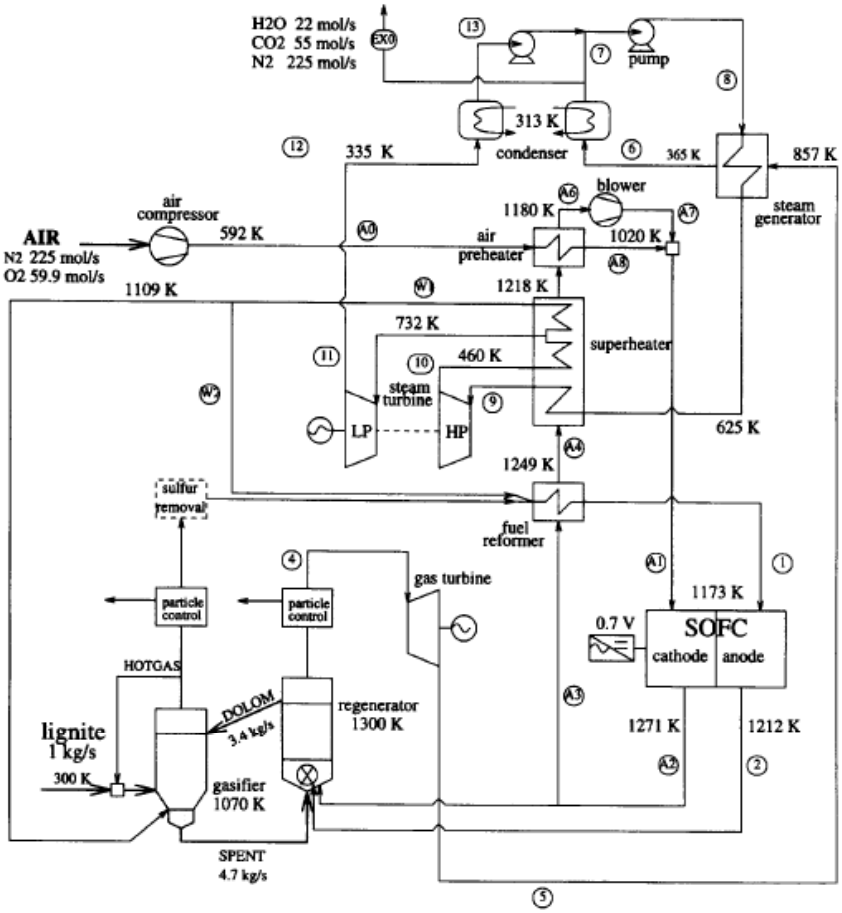

Figure 20 Dartmouth College IGFC Concept

Some unique features of this concept include the elimination of an oxygen air separation unit by using a two-stage gasifier. In addition, the gasifier regenerator stage is partially fueled by the anode exit gas and cathode exit gas. While the efficiency of 63% is significant, analysis as to the amount of air utilization and subsequent air temperature rise in the SOFC is relatively high. Also, the % sulfur capture in the dolomite is assumed to be essentially 100%; it is not known at this time whether this is a realistic assumption. This concept also does not capture CO_2.

2002 Fuel Cell Handbook Concept: Figure 21 gives a schematic taken from reference 18. Characteristics of this concept include the following:

Gasifier:	
Type:	Destec entrained bed
Operating Pressure	19 Atm
Temperature	1043 C (gas exit)
Air Separation	Cryogenic
Gas Cleanup	
Gas cooling	Radiant heat exchanger
Sulfur	Transport, high temperature
Temperature	593 C
Polishing	Zinc oxide
SOFC, High pressure	
Pressure l	18 atm
Cathode Air Temperature In	579 C
Air utilization	25%
Fuel utilization	90%
Cell voltage	0.69
SOFC, Low pressure	
Pressure	4 atm
Cathode Air Temperature In	645 C
Air utilization	34%
Fuel utilization	90%
Cell voltage	0.69
Gas Turbines	
HP pressure	15 atm
LP inlet temperature	979 C
LP pressure	3.3 atm
LP inlet temperature	982 C
Steam Turbines	
High Pressure	100 atm
Reheat Pressure	26 atm

Low pressure 6 atm

Some unique features of this concept include the use of two SOFC stages and gas turbines. By expanding the high-pressure gas from the high pressure SOFC and extracting energy, the gas fed to the lower pressure SOFC is cooled. This turbine exhaust acts as the cathode feed to the low pressure SOFC as it has sufficient oxygen at 14 mole-%. However, it is uncertain at this time whether cathode materials can with stand moisture at these levels (~ 7 mole%). Another unique feature is the use of a high-temperature sulfur removal plus zinc-oxide polishing unit. Also, a unique feature to an IGFC system is the use of a recuperator with a large pressure differential between the hot gas (~ 1 atm) and the cold gas (15 atm). The system efficiency is listed in the reference at 59.7% which, for an entrained gasification system, with a cold gas efficiency almost 6percentage points lower than the BGL gasifier, is significant. An inverter conversion (dc to AC power) efficiency of 0.97 is relatively high. This concept also does not capture CO_2.

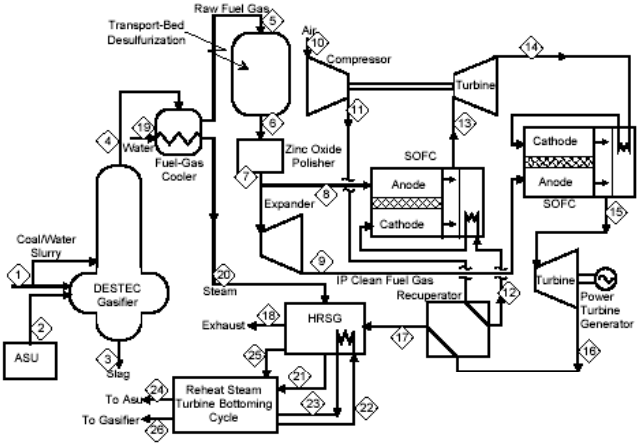

Strm No.	Description	Temp C	Press atm	Mass Flow t/h	Mole Flow kgmol/hr	MW	CH4 %	CO %	CO2 %	H2 %	H20 %	H2S %	N2+Ar %	NH3 %	O2 %	Total %
1	Coal Slurry Feed	18	23.8	151.2	-	NA										
2	ASU Oxygen	179	23.8	83.3	2,583	32.23							5.0		95.0	100.0
3	Slag Waste	93	19.1	11.6	-	NA										
4	Gasifier Effluent	1043	18.6	237.6	12,280	19.35	0.3	42.3	9.5	35.8	9.6	0.7	1.5	0.2		100.0
5	Raw Fuel Gas	593	17.6	237.6	12,280	19.35	0.3	42.3	9.5	35.8	9.6	0.7	1.5	0.2		100.0
6	Desulfurized Gas	593	16.6	236.2	12,280	19.23	0.3	42.3	9.6	35.8	10.3	trace	1.5	0.2		100.0
	Recycle to Gasifier	399	15.0	9.4	491	19.23	0.3	42.3	9.6	35.8	10.3	trace	1.5	0.2		100.0
7	Polished Gas	399	15.0	226.7	11,789	19.23	0.3	42.3	9.6	35.8	10.3	trace	1.5	0.2		100.0
8	HP Fuel Gas	399	15.0	108.8	5,659	19.23	0.3	42.3	9.6	35.8	10.3	trace	1.5	0.2		100.0
9	IP Fuel Gas	221	3.7	117.9	6,130	19.23	0.3	42.3	9.6	35.8	10.3	trace	1.5	0.2		100.0
10	Ambient Air	17	0.98	1,270.1	44,024	28.85			trace		1.1		78.1		20.8	100.0
11	Compressed Air	409	15.1	1,146.2	39,732	28.85			trace		1.1		78.1		20.8	100.0
12	Heated Air	579	15.0	1,146.2	39,732	28.85			trace		1.1		78.1		20.8	100.0
13	HP SOFC Exhaust	979	14.7	1,255.1	43,181	29.07			6.9		7.1	trace	72.1	trace	13.9	100.0
14	HPT Exhaust	645	3.6	1,296.3	44,609	29.06			6.6		6.9	trace	72.3	trace	14.1	100.0
15	IP SOFC Exhaust	982	3.3	1,414.2	48,346	29.25			12.7		12.3	trace	66.9	0.1	8.0	100.0
16	IPT Exhaust	691	1.01	1,477.7	50,547	29.23			12.2		11.8	trace	67.4	0.1	8.6	100.0
17	Cooled Exhaust	573	0.99	1,477.7	50,547	29.23			12.2		11.8	trace	67.4	0.1	8.6	100.0
18	Cycle Exhaust	126	0.98	1,477.7	50,540	29.24			12.2		11.8		67.5		8.6	100.0
19	Gas Cooler Water	306	107.4	244.6	13,580	18.02					100.0					100.0
20	Gas Cooler Steam	317	107.4	244.6	13,580	18.02					100.0					100.0
21	HP Steam	538	99.6	301.4	16,730	18.02					100.0					100.0
22	Cold Reheat	359	29.3	298.4	16,563	18.02					100.0					100.0
23	Hot Reheat	538	26.4	298.4	16,563	18.02					100.0					100.0
24	ASU Steam	538	26.4	3.9	218	18.02					100.0					100.0
25	LP Steam	310	6.1	15.6	865	18.02					100.0					100.0
26	Gasifier Steam	307	5.4	32.0	1,774	18.02					100.0					100.0

Figure 21 Fuel Cell Handbook IGFC Concept

UC Irvine DOE Vision 21 Study: Figure 22 gives a schematic taken from Ref. 18. Characteristics of this concept include the following:

Gasifier:	
Type:	Advanced transport reactor
Operating Pressure	27 atm
Temperature	1052 C (gas exit)
Air Separation	ITM
Gas Cleanup	
Gas cooling	Radiant heat exchanger
Sulfur	85% S captured in calcined limestone
Polishing	Warm gas clean up @ 400C
SOFC	
Pressure	15 atm
Cathode Air Temperature In	471 C
Cathode Air Temperature Ex	979 C
Air utilization	43%
Fuel utilization	85%
Cell voltage	0.69
Gas Turbine	
Inlet pressure	15 atm
Inlet temperature	754 C

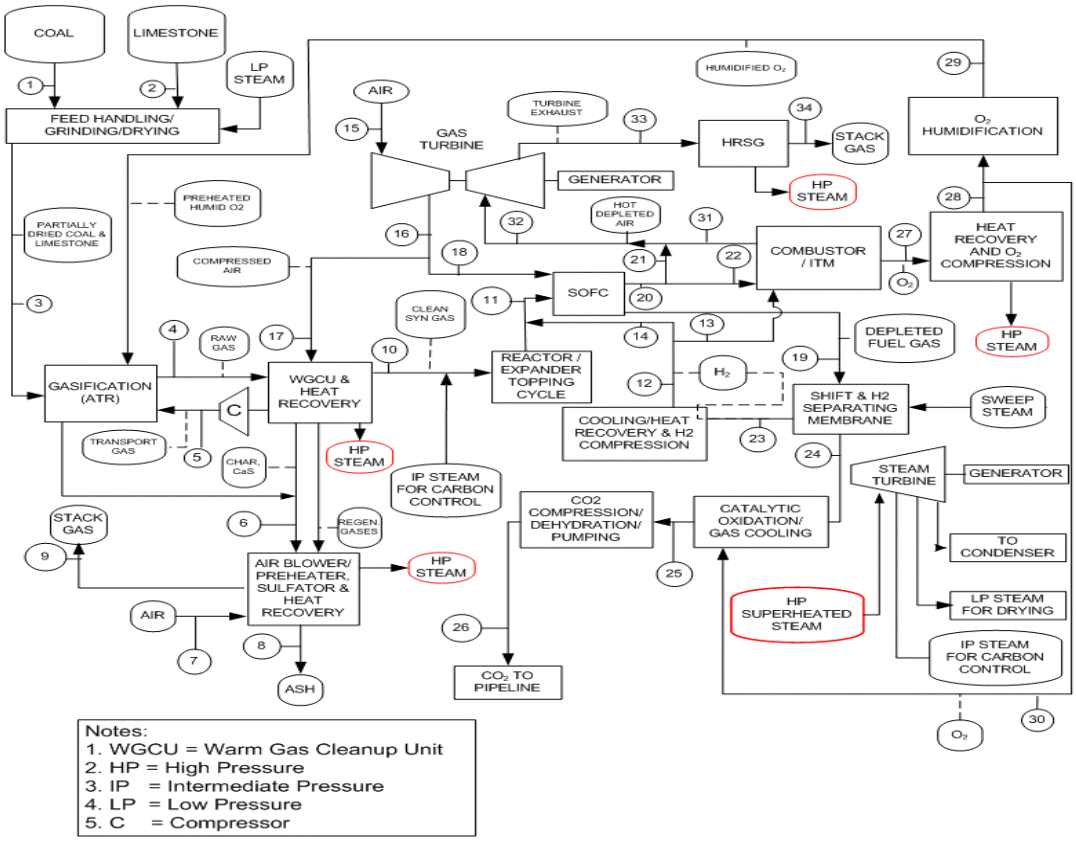

Figure 22 UCI Vision 21 IGFC Concept

Some unique features of this concept include

- The use an advanced transport reactor for the coal gasifier including the use of limestone to capture the majority of the sulfur and the chlorines form the coal
- A warm gas cleanup system to remove the balance of the sulfur and the chlorines
- An ITM for oxygen generation
- A Methanation reactor with an expansion turbine on the syngas prior to feeding the SOFC
- A high-temperature H2 membrane and shift reactor to recycle anode gas and enable a high overall fuel utilization
- Pressurization of the CO_2 to pipeline pressure for sequestration

The system efficiency given in the reference is only 49.6%. However, the concept includes more than CO_2 isolation; the CO_2 is compressed to 140 bar for insertion into a pipeline and eventual sequestration.

Columbia University IGFC Concept: This concept has several unproven components that would need significant development work to test the feasibility, including a very high temperature SOFC. Figure 23 gives a schematic taken from References 22 and 23. Notable characteristics of this concept include the following:

Gasifier: This gasifier, while not novel in itself as a gasifier, is novel for an IGFC concept. Hydrogasification is a reaction of pulverized coal with hot, high-pressure hydrogen for a short period of time. The hydrogasification reactions are:

$$C+2H_2 \rightarrow CH_4$$

The optimal conditions for this process are:

- Temperature range of 1000°F (538°C) to 2000 °F (1076°C)
- Hydrogen partial pressure of 500 to 3000 psi (34 to 204 atm)
- Particle residence time of 0.05 to 10 seconds

Recent studies indicated that the reaction could reach 90% completion at 926°C and 69 atm.

Reformer/CO_2 Acceptor:

Hydrogen makeup for the hydrogasifier occurs in this reformer/CO_2 acceptor reactor. It is not known how well this unit will work as the CaO/CACO3 is continuously cycled. The CO_2 acceptor reaction is:

$$CaO + CO_2 \rightarrow CaCO_3$$

Calciner:

Most carbon sequestration techniques involve a reaction of a concentrated carbon dioxide stream with an oxide to form carbonate. Calcium and magnesium oxides are the most studied acceptors of CO_2.

A combination of the two such partially calcined dolomite (MgO*CaO) has been shown to be successful.

High temperature SOFC: the operational temperature (1200 °C) and a very high conversion efficiency (70% of reacted H2 heat) to dc power was assumed. The high operating temperature allows waste heat from the SOFC to be utilized in the calciner which requires a temperature of 1000C.

With the very aggressive assumptions of the SOFC, this IGFC efficiency could approach 60% based on preliminary conceptual modeling.

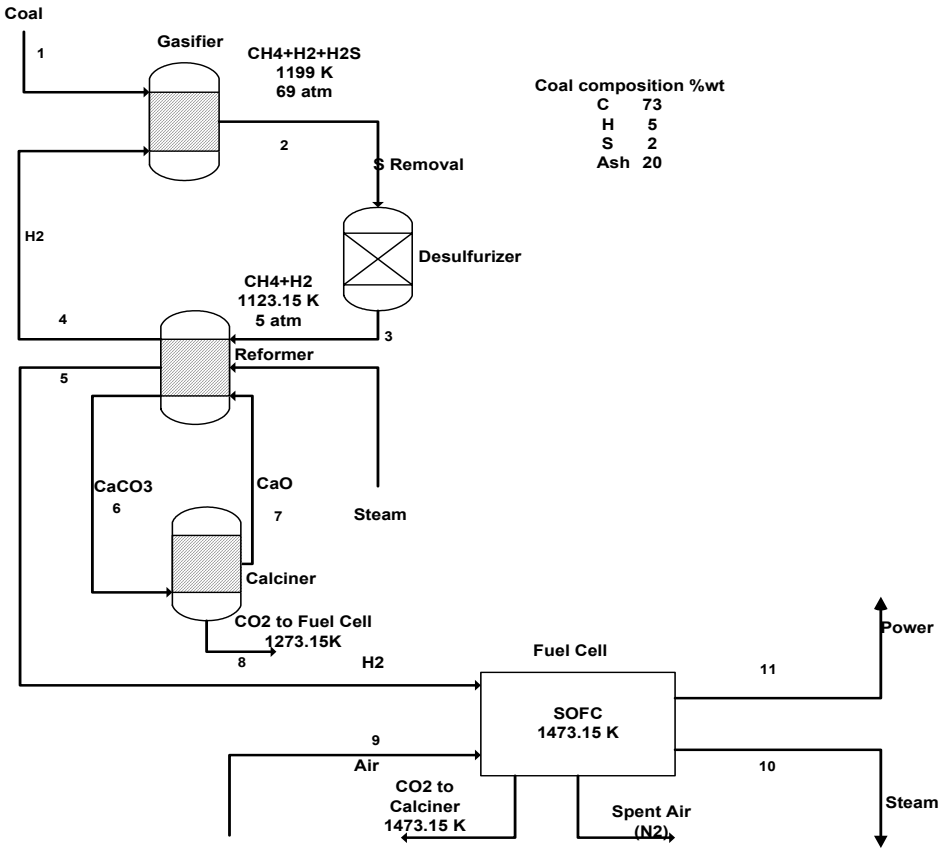

Figure 23 Columbia University's Hydro-gasification Zero Emission Coal Power Plant Concept

Conventional State-of-the-Art Entrained Bed Gasifiers: Entrained-bed coal gasifiers that are considered ready for use in an integrated gasification combined cycle plant (IGCC) today would include the following:

- GE (formerly ChevronTexaco)
- E-Gas (or Destec, Conoco-Phillips)
- Shell

Studies by DOE (22) have indicated in an IGCC plant, the system efficiencies range in the low- to mid-forty-percent efficiency range (HHV coal to AC power) assuming cold-gas cleanup technology is used. A top-level analysis was performed replacing the BGL gasifier with a GE (Texaco) entrained bed gasifier, assuming similar baseline components downstream of the gasification/cleanup systems are employed. The analysis also assumed the inclusion of ITM technology to generate oxygen. The system efficiency is estimated to be slightly lower than 50%.

In addition to the above concepts, several technologies were identified that, if inserted into an IGFC system could have potential efficiency gains include:

- The use of GE's Unmixed Fuel Processor (UFP) for coal-based H2 production in a IGFC configuration (19)
- The use of a mid-temperature membrane to separate CO_2 from a H2 rich stream
- The use of a gasifier designed for higher CH4 yield, such as a BI-GAS gasifier previously under development by the DOE (20)

1.4.3.3 System Concept Down Selection

The most promising concept from the brainstorm concepts will be chosen for further evaluation. Criteria for down selection are to be identified. Factors to consider are:

- Highest efficiency
- Maturity of technologies
- Risk in achieving assumed performances
- Cost

1.4.3.4 Model Development

To further evaluate the down selected concept, a top-level model is under development using ASPEN PLUS. It will include all the major component islands with the ability to vary important performance parameters to determine the effects on system efficiency.

2 TASK 2.4 – CELL SCALABILITY

2.1 Introduction

The objective of this task is to demonstrate cell area scaleup based on the tape calendering method. Both theoretical analysis and experimental work will be conducted. The theoretical analysis will involve literature search to determine fundamental limitations, if any, on the size that can be sintered. Experimental work as well as theoretical studies will be performed to identify the key process parameters that affect cell scalability. These key factors will be optimized to demonstrate process scaleup to large area cells (> 10" diameter). Testing will be conducted on representative large area cells to determine their performance under typical hybrid operating conditions.

2.2 Background

The tape-calendering method was used to fabricate the cells. Figure 24 shows the basic tape-calendering sequence for producing a thin electrolyte supported on an anode support. In this process, the starting materials (YSZ electrolyte, NiO/YSZ anode support electrode, organic binders, and plasticizers) are mixed in a high-shear mixer. The heat generated by the mixing process softens the organics to form a homogeneous plastic mass. Each plastic mass is then rolled to produce a flexible sheet on the order of 0.25 to 2.5 mm thick. The electrolyte and anode tapes are then laminated together to form a

bilayer and subsequently rolled to reduce the thickness of each layer. Another anode tape is added to the bilayer and again rolled to a thin tape. The addition of anode tapes has the effect of reducing the electrolyte thickness while keeping the bilayer at a handleable thickness. Such process is repeated until the desired thickness of electrolyte is reached. At this point, the bilayer is cut to the desired shape and size. The green tape is then fired at elevated temperatures in an air atmosphere to sinter the bilayer tape. The cathode is then screen printed on the electrolyte surface of the sintered bilayer to produce a complete cell (Figure 24).

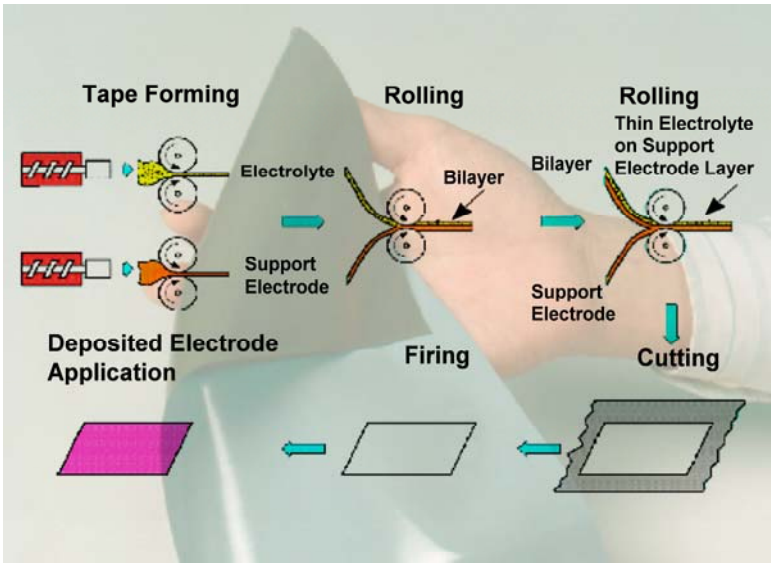

Figure 24 Schematic showing the process steps in the tape calendering process

Fabrication of the SOFC ceramic components by tape calendering utilizes the basic principles and processes of ceramic engineering to meet the structural and material requirements for a high-performance SOFC. Each of the components of the ceramic cell has different requirements. A thin, dense electrolyte is crucial as a gas separator membrane in the fuel cell and for high performance as the oxygen ion conductor. In the electrodes, however, a porous structure is required to reduce polarization losses. The anode has three roles, electrochemical, structural and gas delivery to the electrochemical reaction sites. Optimum electrochemical properties are only needed near the anode/electrolyte interface, thus a thin layer with these properties can be designed into fabrication process to meet these requirements. The structural and gas transport requirements are met through a multilayer anode approach. By incorporating layers of increasing pore size on top of the electrochemical layer the structural needs can be traded off with the gas transport need to create a multilayer anode.

Some of key requirements that the fabricated cells must meet are: a) strength-cell should be able to withstand handling and stacking stresses; b) flatness-flatter cells are better to facilitate to provide uniform contact during stacking; and c) performance-cell material and microstructure should be able to provide high performance in order to

reduce overall cost. As shown in figure 1, cells sizes of 16cm (6.3”) meeting the above requirements are routinely fabricated at GE HPGS.

State-of-the-art in cell size reported for planar stacks is as follows: Mitsubishi Heavy Industries, Japan (20 cm x 20 cm); Fuel Cell Energy, USA (15 cm or 5.9 inch diameter); Julich, Switzerland (20 cm x 20 cm); Ceramic Fuel Cells Limited, Australia (13 cm diameter); General Electric, USA (20.32 cm or 8 inch diameter); and Indec, Switzerland (15.6 cm or 6.13 inch diameter). (21). As evident from the above information, the focus of this work, i.e., fabrication and testing of cell sizes greater than 10” diameter, would be beyond that demonstrated to date in SOFC planar cell technology.

2.3 Large Cell Fabrication

Initial attempts on large cell fabrication involved rolling larger tapes of baseline composition and firing the cells in the standard manner used for baseline tapes. However, two successive attempts on all 6 tapes resulted in severe cracking of the type typically seen in early stage failures (Figure 25).

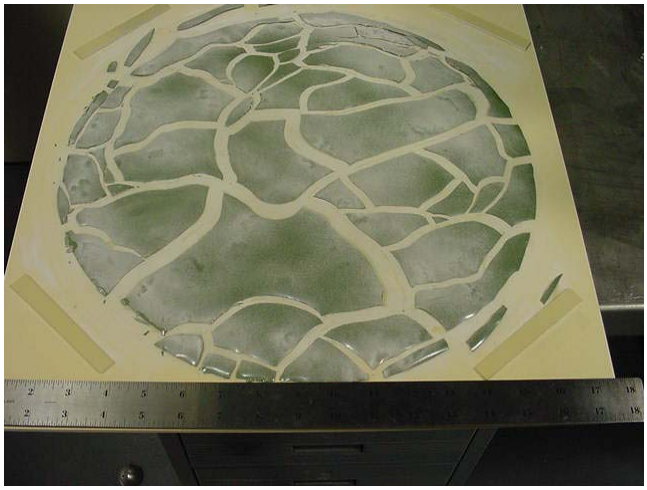

Figure 25 Photograph illustrating failures during firing of a large cell

It was also decided to prepare some tapes with a modified composition based on the results from experiments and prior experience. Key processing steps were also modified. When these changes were incorporated, the first firing run showed excellent results (Figure 26).

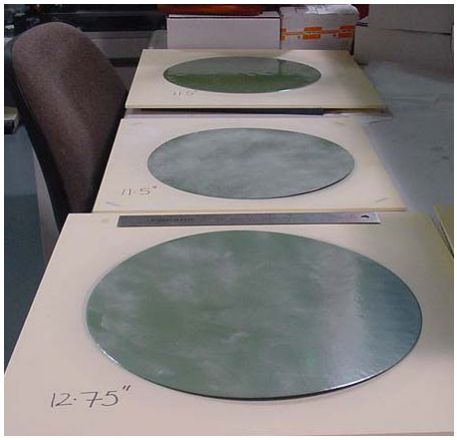

Figure 26 Photographs of successfully fired large cells up to 12.75" in size.

After the first firing run demonstrated that 12" bilayers can be fired, additional runs were made to ensure the repeatability of firing step. The average firing yield on 20 cells from 5 runs was about 67%.

One of the other major issues encountered was the breakage of cells either during firing or in handling due to defects. A distinctive feature of these defect-related failures was that the cell broke into two-or more large pieces (Figure 27). Visual and optical microscopic examination of the cross-section of cells broken in this configuration revealed large particles with slight bluish hue. SEM examination of the cross-section revealed that these defects were about 100-200 microns in size and were rich in alumina. It is possible that the bluish color observed may be due to the formation of a nickel aluminate compound.

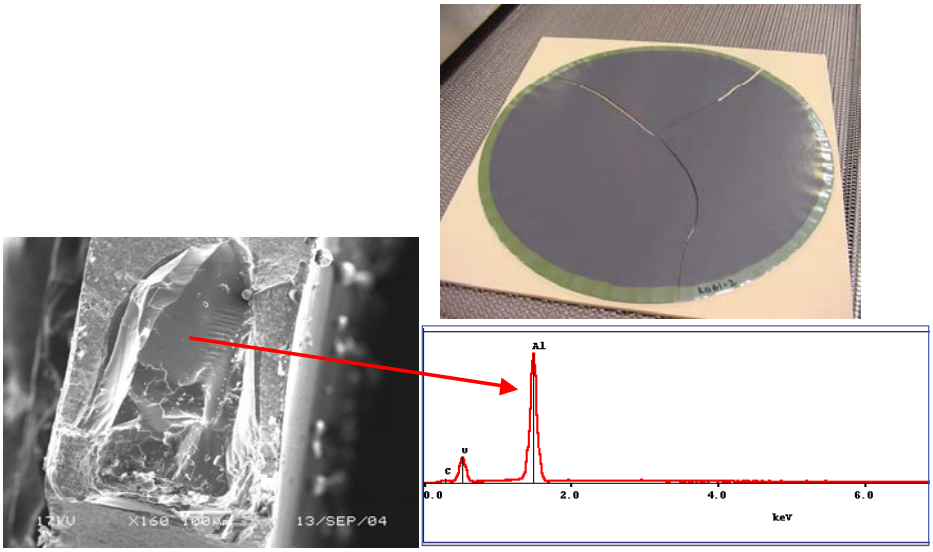

Figure 27 Surface view of a broken cell and x-sectional view indicating the presence of a defect and its chemical composition

Possible source of these defects include contamination in the raw material or particles in ambient atmosphere. A procedure was instituted to reduce the possibility of raw material contamination with large particles. Subsequent cells firing runs with the tape made using the sieved powders did not exhibit the defect-related failures. These results, though preliminary, do indicate the potential process improvements that can be made by addressing issues related to special cause defects.

2.4 Large Cell Performance Test

During this reporting period, two large-area cells were tested by using radial sealless single cell test vehicle to assess the capability of testing large area cell in our current test vehicle and facility, and evaluate the effects of hybrid environment on the performance of large cell, particularly, the effects of pressure on cell temperature distribution, and cell flow uniformity.

2.4.1 DH02: 11-3/4 Inch Diameter Radial Seal-less Cell Module Test

2.4.1.1 DH02 Test Setup

The 11-3/4" single cell module was based on radial sealless design that was developed at GE HPGS. It should be understood that the assembly process of the large-area cell is not a mature process at this stage and it has been faced with a number of technical challenges so far. The assembled large-area single cell module is shown in Figure 28. The cell active area of the single cell module is 532 cm^2.

In order to mimic the hybrid SOFC operation conditions, two preheaters that compose of a serpentine design of ¼" tubing were used to heat the air and fuel to the SOFC operating temperature under pressurized conditions. Both air and fuel preheaters were sized based on their maximum flow rates, the air and fuel could be heated up to 750°C at the single cell module inlets.

Figure 28 Assembled Large-area Single Cell Module with 532 cm^2 Active Area

2.4.1.2 DH02 Test Results

The 11-3/4" radial sealless single cell module was heated up to 800 ◦C for normal SOFC operations. The anode reduction was started after the single cell module temperature reached 800 ◦C. The test sequence for the 11-3/4" radial sealless single cell module is listed in Table 10.

Table 10 11-3/4" Radial Sealless Single Cell Module Test Sequence

- Initial polarization curve at fixed flows with dilute hydrogen (64% H_2/balanced with N_2) (at 14.7 psia. and 800 °C);
- Hold for 20 hours under constant current for conditioning (at 14.7 psia. and 800 °C);
- Polarization curve at fixed flows with dilute hydrogen (at 14.7 psia. and 800°C);
- Polarization curves at fixed fuel utilization with dilute hydrogen (at 14.7 psia. and 800°C);
- Polarization curves at fixed fuel utilization with simulated SR fuel (at 14.7 psia. and 800°C);
- Polarization curve at fixed flows with dilute hydrogen (at pressurized condition and 800°C);
- Polarization curves at fixed fuel utilization with dilute hydrogen (at pressurized condition and 800°C);
- Polarization curves at fixed fuel utilization with simulated SR fuel (at pressurized condition and 800°C);
- Polarization curves at fixed fuel utilization with dilute hydrogen (at pressurized condition and different temperature);

a. Cell performance with diluted hydrogen fuel at fixed flow rate

The performance of 11-3/4" radial sealless single cell module running on fixed flow with 64% H_2 fuel stream is shown in Figure 29 at different pressurization levels. The peak power density at ambient pressure (14.7 psia) was measured to be 152 mW/cm^2 and it reached 214 mW/cm^2 at 61.5 psia. From ambient pressure condition, the peak power density is calculated to increase by 19% at 29.4 psia, 34% at 44.1 psia and 41% at 61.5 psia, respectively. Under low fuel and air utilization and high cell temperature (about 845 °C), the peak power density at 61.5 psia reached 253 mW/cm2.

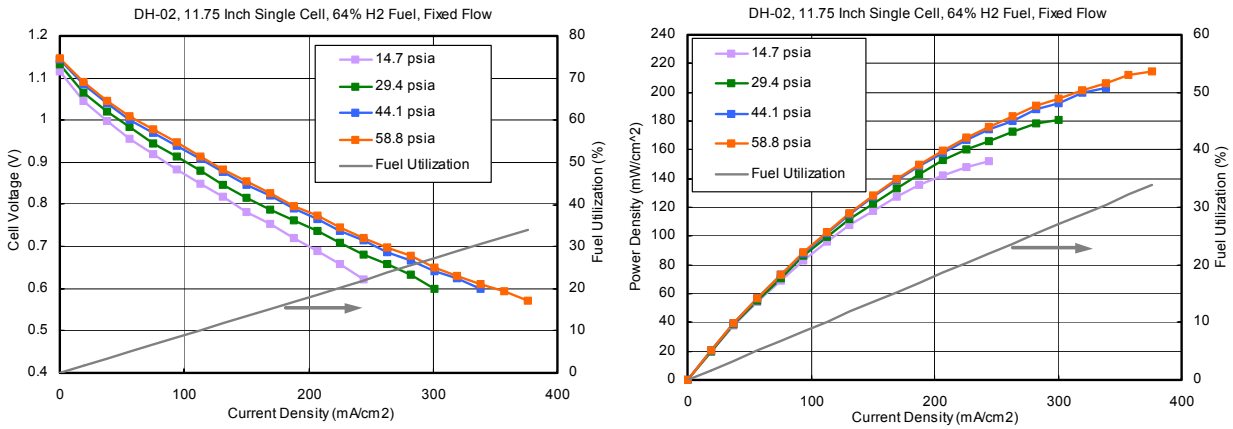

Figure 29 Performances of the 11-3/4" Radial Sealless Single Cell Module, DH-02 as a Function of Operation Pressure with 64% H_2 and Fixed Flow at 800°C

b. Effects of fuel composition (64% H_2 vs. simulated SR fuel steam)

The performance of 11-3/4" radial sealless single cell module running on 64% H_2 fuel stream was compared with that on SR fuel in Figure 30. The peak power density measured on SR fuel was 89 mW/cm^2 and this is way lower than that measured on 64% H_2 fuel stream (152 mW/cm^2).

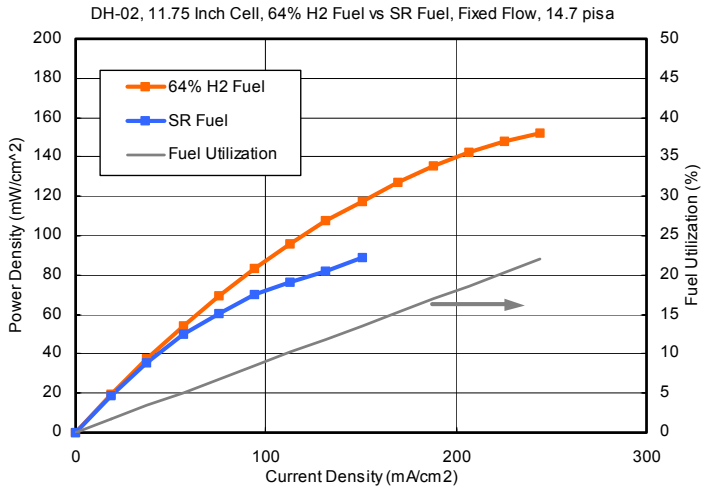

Figure 30 Performances of the 11-3/4" Radial Sealless Single Cell Module, DH-02 with Diluted H_2 and SR Fuel and Fixed Flow at 800°C

c. Post-mortem test and root cause analysis

Post-mortem test was performed after the first 11-3/4" radial sealless single cell module, DH-02 test to find the evidences that may lower the stack performance. Crack and burning marks were found about 1 inch away from the cell perimeter. A

root cause analysis was performed to identify causes of the cell crack and high cell ASR. Recommended actions to mitigate the risks of cell crack and high cell ASR were also identified.

2.4.2 DH05: 12.5 Inch Radial Seal-less Single Cell Module Test

2.4.2.1 DH05 Test Setup

To improve the performance of large-area radial sealless single cell module, reduce the ASR of the module, a 12.5" radial sealless single cell module, DH05 was assembled by using Ni foam as the anode flow field and reducing the diameter of the endplate to about 12.3 inch so that the edge of the 12.5" cell can hang out of the flow field and avoid the cell crack induced by touching the endplate (see Figure 36). The assembled large-area radial sealless single cell module, DH-05 is similar to 11-3/4" radial sealless single cell module, DH-02. The cell active area of the 12.5" radial sealless single cell module is 670 cm^2. Preheaters that compose of a serpentine design of ¼" tubing were also used to heat the air and fuel to the SOFC operating temperature.

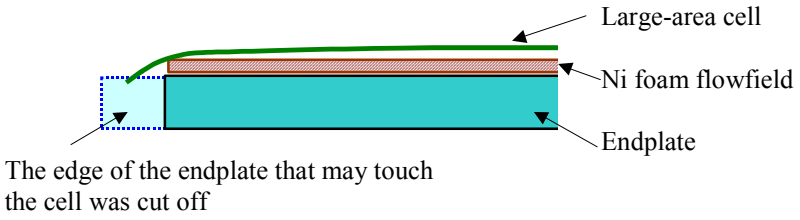

Figure 31 Reduce the Diameter of Endplate to Avoid the Cell Crack Induced by Touching Endplate

2.4.2.2 DH05 Test Results

The 12.5" radial sealless single cell module was heated up to 800 ◦C for normal SOFC operations. The anode reduction was started after the single cell module temperature reached 800 ◦C. The test sequence for the 12.5" radial sealless single cell module is listed in Table 10.

a. Cell performance with diluted hydrogen fuel at fixed flow rate

The power density curves of 12.5" radial sealless single cell module, DH05, running on fixed flow, 64% H_2 fuel and SR fuel stream, respectively, are shown in Error! Reference source not found.. The peak power density of DH-05 cell on 64% H_2 fuel stream was higher than that on SR fuel stream by around 34 – 50% throughout the whole pressurization levels employed.

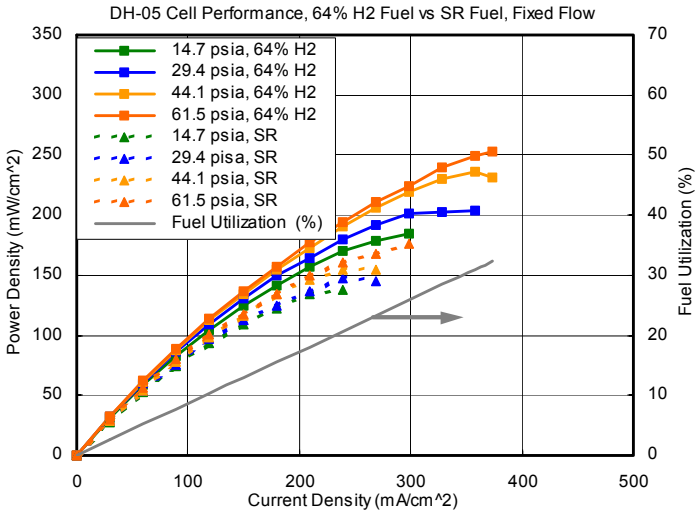

Figure 32 Performances of the 12.5" Radial Sealless Single Cell Module, DH-05 with Diluted H_2 and Simulated SR Fuel at Fixed Flow at 800°C

Compared with the performance of 11-3/4" Radial Sealless Single Cell Module, DH-02, the DH-05 showed approximately 20% increase in power density at fixed flow with 64% H_2 fuel stream (see Figure 33). This improvement might be attributed to (i) "flatter" DH-05 cell compared to DH-02 cell since there is significant improvement in the preparation of "flatter" large-area cells, which is explained in detail in other part of this report, and (ii) the modified assembly processes that is expected to have reduced the ohmic resistance originating from poor contact between the electrode surface and flow field. Along with the improvement in cell and assembly processes, the thickness of Ni foam for anode flow field was reduced in DH-05 cell assembly. This reduced Ni foam thickness translates to increased pressure drop along the radial fuel flow path and is considered to promote convectional mass transfer of fuel species within anode flow field.

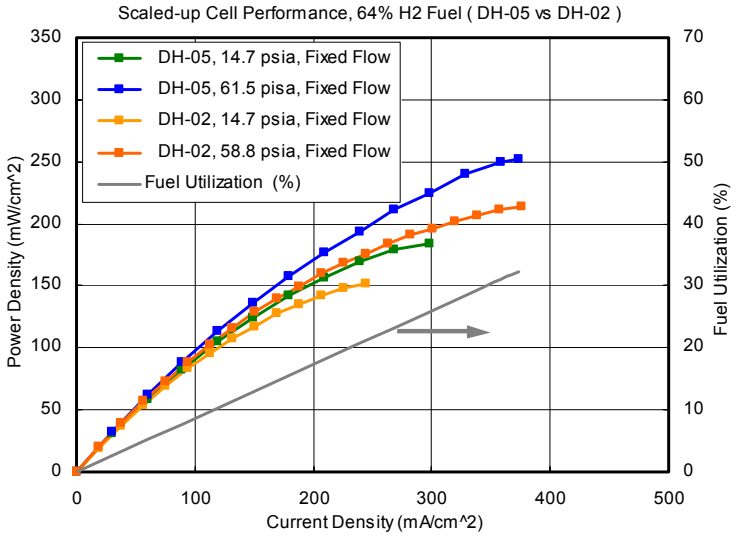

Figure 33 Performances of the Large-area" Radial Sealless Single Cell Module, DH-05 and DH-02 with Diluted H_2 and Fixed Flow at 800°C

3 TASK 2.5 – STACK HYBRIDIZATION

The objective of this task is to demonstrate operation of planar SOFC stacks and their operating characteristics under hybrid environment and assess scalability of stack design. SECA derived technology will be leveraged in this task. The work will focus on stack testing of various sizes under hybrid conditions, such as temperature, pressure, and gas composition, which are critical to the development of megawatt class hybrid demonstration systems. Stack performance as a function of fuel utilization will be determined. Analysis of design features that influence stack reliability, performance, and scalability (area and height) will be performed. The dynamic performance of stacks under hybrid conditions including startup and shutdown will be evaluated. Designs and operating procedures to facilitate stack scaleup will be identified.

A 2-cell and two 5-cell stacks were tested in hybrid conditions during this report period. All three stacks are circular half sealed design and with 142 cm^2 active area. The performances of the stacks as a function of pressure, temperature, fuel utilization, and fuel composition have been evaluated to meet the requirement of the task. The results of these tests are summarized below.

3.1 DH01: 2-Cell Stack Test

During this reporting period, a 2-cell stack, DH-01, was tested to evaluate the effects of hybrid environment on the performance of SOFCs, particularly, the effects of pressure on cell seal, cell temperature distribution, and cell flow uniformity since the 2-cell stack contains all of the design features of the n-cell stack. The functionalities and safety of SOFC pressurized test stand were also checked during this test.

3.1.1 DH01 Test Setup

The 2-cell stack was based on the stack that was designed for SECA program. In order to mimic the hybrid SOFC operation conditions, preheaters that compose of coils of $^1/_8$" tubing were used to heat the air and fuel to the SOFC operating temperature under pressurized conditions. The assembled 2-cell stack is shown in Figure 28. The cell active area of the 2-cell stack is 142 cm^2.

Figure 34 Assembled 2-cell stack with 142 cm^2 active area per cell

3.1.2 DH01 Test Results

The 2-cell stack was heated up to 900 ◦C for curing the manifold, anode and cathode cell seals. Then, the stack was cooled down to 800 ◦C for normal SOFC operations. The anode reduction was started during the stack heating up when stack temperature reached 600 ◦C. The test sequence for the 2-cell stack is listed in Table 11.

Table 11 2-Cell stack test sequence

- Initial polarization curve at fixed flows with dilute hydrogen (64% H_2/balanced with N_2) (at 14.7 psia. and 800°C);
- Hold for 20 hours under constant current for conditioning (at 14.7 psia. and 800°C);
- Polarization curve at fixed flows with dilute hydrogen (at 14.7 psia. and 800°C);
- Polarization curves at fixed fuel utilization with dilute hydrogen (at 14.7 psia. and 800°C);
- Polarization curves at fixed fuel utilization with simulated SR fuel (at 14.7 psia. and 800°C);
- Polarization curve at fixed flows with dilute hydrogen (at pressurized condition and 800°C);
- Polarization curves at fixed fuel utilization with dilute hydrogen (at pressurized condition and 800°C);
- Polarization curves at fixed fuel utilization with simulated SR fuel (at pressurized condition and 800°C);
- Polarization curves at fixed fuel utilization with dilute hydrogen and simulated SR fuel (at pressurized condition and different temperature);

a. Effects of fuel composition (64% H_2 vs. simulated SR fuel steam)

The performance of the 2-cell stack, DH-01 running on diluted hydrogen fuel (64% H_2, balanced with N_2) and simulated steam reformate (SR) fuel stream are shown in Figure 29. The fuel flow rate was fixed throughout the whole current density range and therefore, fuel utilization increases linearly with current density as shown in Figure 29. The performance curves (I – V curves) were measured at both ambient pressure (14.7 psia) and elevated stack operation pressure (58.5 psia). Cells running on 64% H_2 fuel stream show cell voltages higher than SR fuel stream by approximately 0.5 Volt (both ambient and pressurized condition) when compared at same current density. Pressurization of the stack operation pressure from ambient pressure to 58.8 psia raises the cell voltages and the voltage gain through pressurization is seen generally to grow with current density (compare solid line and dotted line in Figure 29). It should be noted that the open circuit voltage of cells running on SR fuel is raised (from 0.971V to 1.026V on cell #1 in Figure 29) when the stack was pressurized from ambient pressure to 58.8 psia. This increase in open circuit voltage is in good agreement with thermodynamic prediction. With SR fuel stream, thermodynamic calculation predicts that pressurization decreases equilibrium O_2 composition in fuel stream and leads to increased open circuit voltage.

The low cell voltage (or performance) observed with SR fuel stream vs. 64% H_2 fuel stream can be explained primarily by internal reformation. The SR fuel stream contains 13.6% CH_4 (the CH_4 slip comes from steam reformer for external reformation), and the CH_4 content is dropped to less than 1.0% through internal reformation within SOFC anode compartment (the high conversion of CH_4 through internal reformation within SOFC anode compartment has been measured in separate studies at HPGS and is close to thermodynamic equilibrium predictions). The occurrence of this internal reformation, which is highly endothermic (approximately 205 kJ/mole), lowers the stack temperature (especially cell temperature) and leads to reduced cell voltages. The local cell temperature inside the stack is anticipated to vary widely and more precise measurement of local cell temperature is required to clearly understand internal reformation driven local cooling effect.

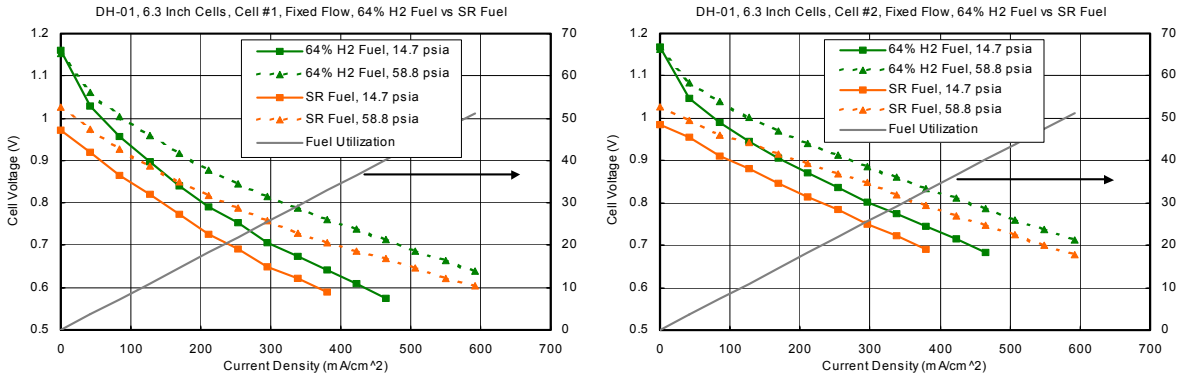

Figure 35 Performances of the stack, DH-01 with diluted H_2 and steam-reformate fuel

b. Effects of fuel utilization

Cell performances were also measured with fixed fuel utilization. Fuel flow rates were controlled at given current densities to match fuel utilization specification (i.e., fuel flow increases linearly with current density). Figure 30 shows cell voltages measured with 75% fuel utilization on 64% H_2 fuel and simulated SR fuel streams, respectively. The starting current density of these measurements was higher than 300 mA/cm^2 because the requirement of the low fuel flow rate for low current density reached the limitation of the mass flow controllers.

As shown in Figure 30, the voltage gain through pressurized operation was most significant at initial pressurization level (e.g., when going from 14.7 psia to 29.4 psia), the high pressurization level (e.g., from 44.1 psia to 58.8 psia) did not raise cell voltages appreciably (less than 20 mVs). It is seen that 64% H_2 fuel maintains higher cell voltage over simulated SR fuel at 75% fuel utilization condition.

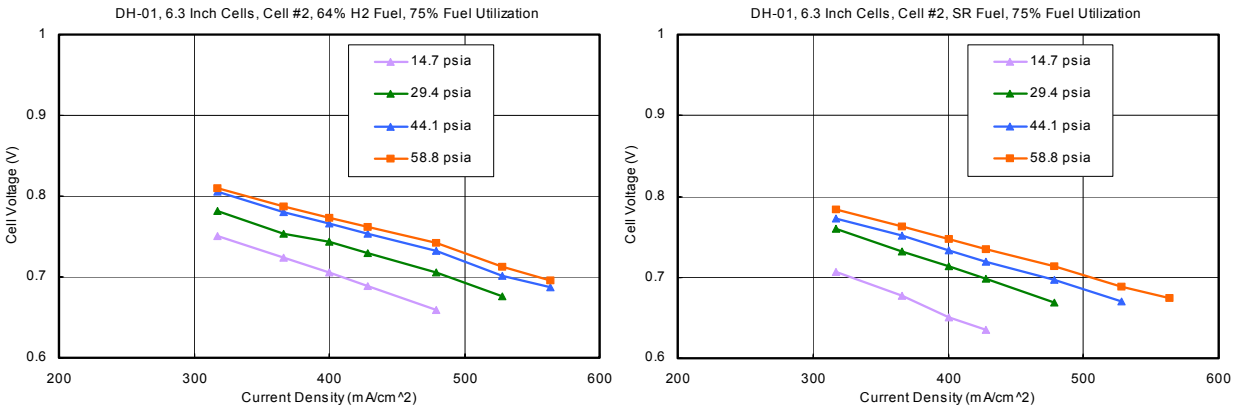

Figure 36 Performances of cell #2 of DH-01 stack at 75% fuel utilization with dilute H_2 and steam reformate fuel

The I-V curves of cell #2 shown in Figure 30 are plotted for power density in Figure 37. With 64% H2 fuel stream, the power density of cell #2 at ambient pressure is measured to be 0.32 mW/cm^2 and it reaches 0.39 mW/cm^2 at 58.8 psia. With simulated SR fuel stream, power density at ambient is measured to be 0.27 mW/cm2 and 0.38 mW/cm2 at 58.8 psia, respectively. The increases of power density with simulated SR fuel stream from ambient pressure (14.7 psia) is calculated to be 18% at 29.4 psia, 31% at 44.1 psia, and 40% at 58.8 psia.

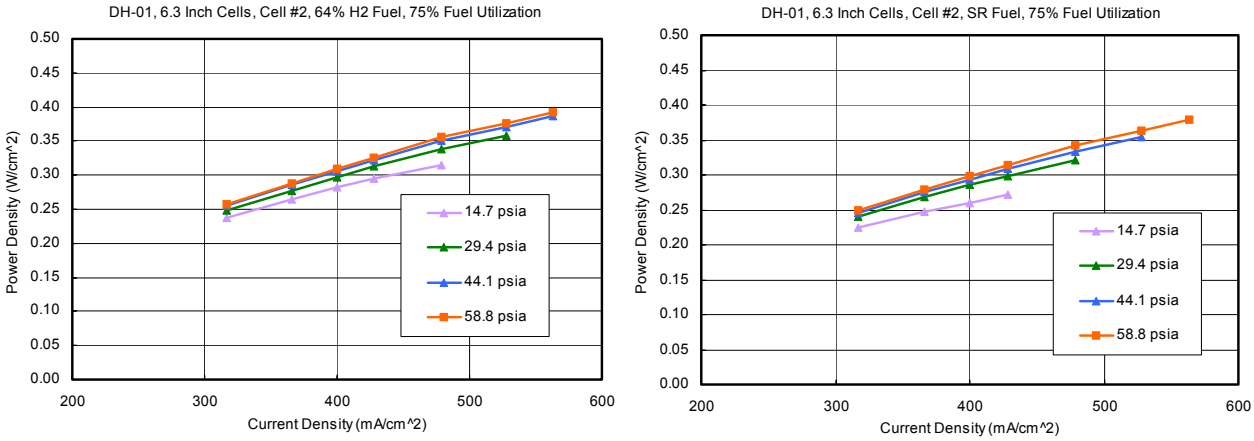

Figure 37 Power Density of Cell #2 of the stack, DH-01 at 75% fuel utilization with diluted H_2 and steam reformate fuel

c. Effects of SOFC operation temperatures

The effect of temperature on SOFC performance was measured under pressurized condition (58.8 psia). Figure 37 shows cell performance on 64% H_2 fuel at 75% fuel utilization. Vessel temperature was maintained at 750°C, 800°C and 850°C, respectively, during performance measurement.

As shown in Error! Reference source not found., stack operation temperature brings about noticeable change in cell performance. When compared to power density at 800°C for cell #1, 13% increase in power density was observed at 850°C and 27% drop in power density was observed at 750°C, respectively.

The effect of temperature on cell performance could also be clearly observed with simulated SR fuel stream as shown in Figure 38. The power density measured at 850°C on cell #2 running on simulated SR fuel stream (Error! Reference source not found.) reached 0.41 W/cm2 and this power density translates to 62% increase in power density over that (0.25 W/cm2) at 750°C.

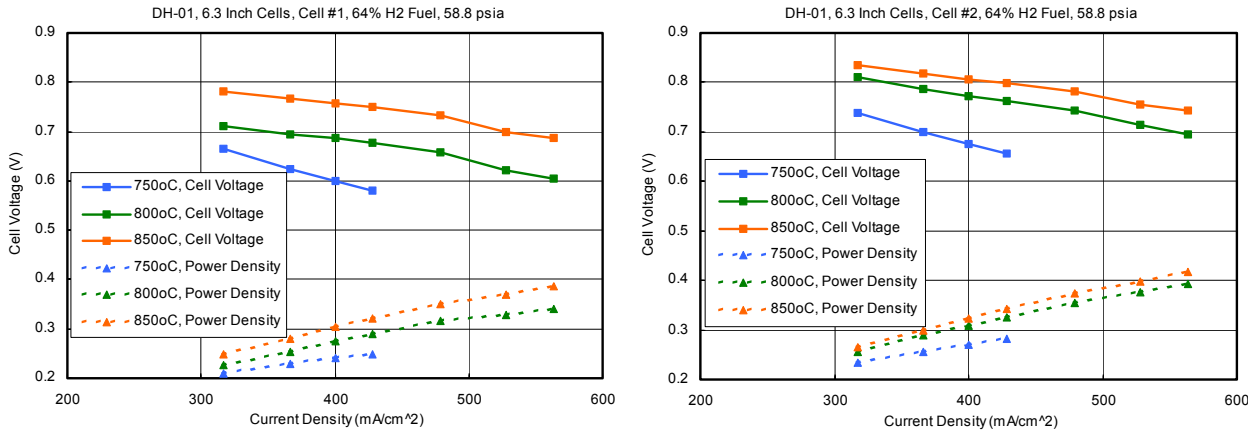

Figure 38 Performances of the stack, DH-01 as a function of temperature at 75% fuel utilization with diluted H_2

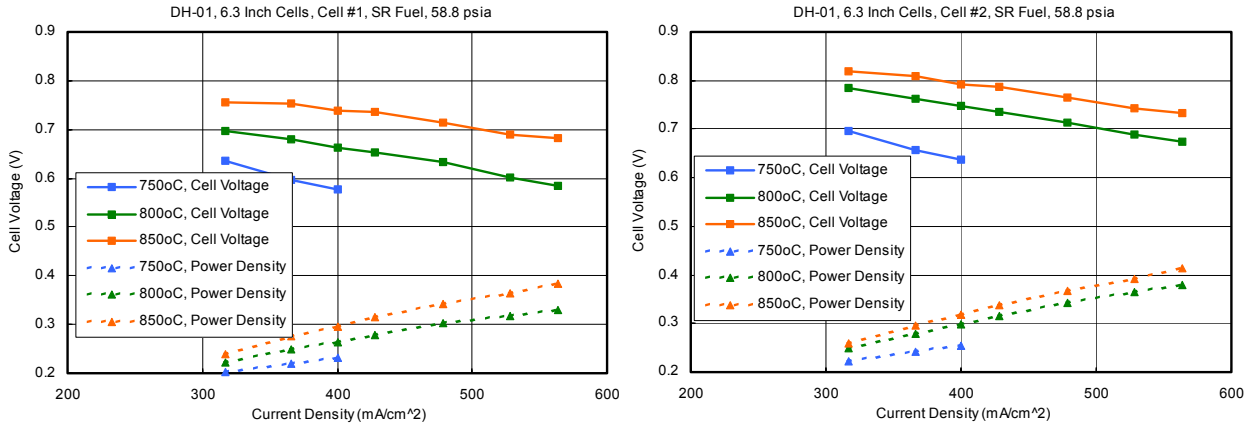

Figure 39 Performances of the stack, DH-01 as a function of temperature at 75% fuel utilization with simulated steam reformate fuel

d. Stack performance degradation

DH-01 stack has been tested for over a week period of time and has gone through 6 pressure cycles. During the test period, cell performance at fixed test condition (64% H_2 fuel stream, fixed flow, 800°C, 14.7 psia) was repeated to check stack performance day-to-day stability. The cell voltages measured at certain current densities are shown in Figure 31. So far, it was observed that pressure cycle (pressurizing and de-pressuring of the stack) does not apparently affect individual cell stability. However, it is too early to quantify cell stability at this stage because of limited test data. In this task, not much attention has been given to long-term cell stability issue. For clear understanding of cell stability issues within the framework of hybrid system configuration, more stability test with long-term time frame is considered necessary.

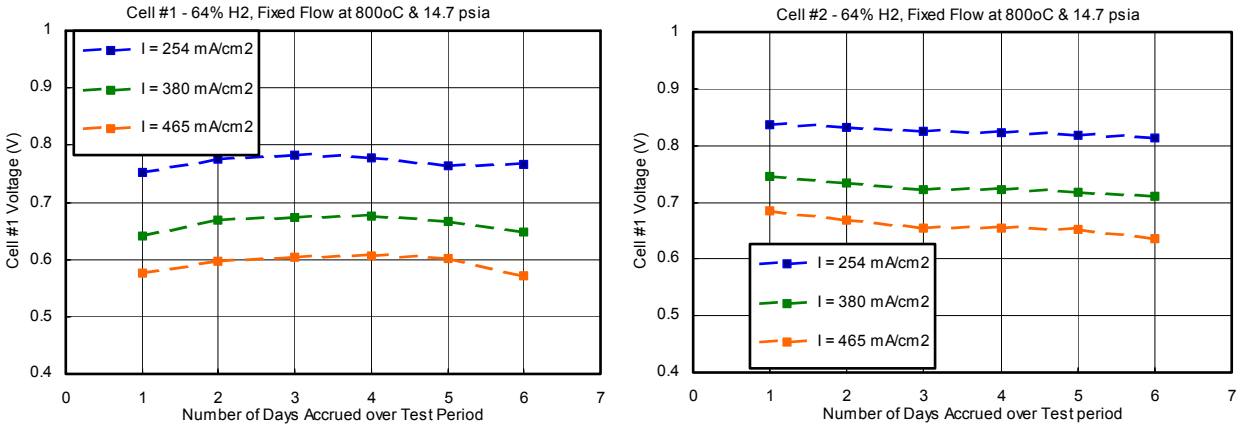

Figure 40 Performance stability of the stack, DH-01 with dilute H_2 at 800°C and 14.7 psia

3.2 DH06: 5-Cell Compliant Feed Tube Stack Tests

After the successful test of the 2-cell stack, two 5-cell stacks, DH-06 and DH-07, were tested under hybrid conditions. The purpose of the two 5-cell stack tests was to evaluate the performance of the SOFC stack as a function of pressure, temperature, and fuel utilization and the capability of the compliant feed tube manifold system (compliant feed tube and manifold sealant) at hybridization conditions. Simulated steam-reforming fuel was used in the tests.

3.2.1 DH06 Test Setup

Because the stack design showed several major risks, such as manifold seal leakage, manifold shorting, and tolerance stack-up for interconnect during the stack test, the compliant feed tube stack design that was also developed under SECA program was used in the 5-cell stack tests. The advantages of the compliant feed tube stack design are (i) using feed tubes replace the bellows to provide the compliancy between stack core and manifold, and avoid the loss of the compression on manifold due to the bellows material anneals at the SOFC operation temperature; (ii) capable of presealing cell to interconnect and reducing cell that allow inspection of the cell crack, cell shorting, cell seal, pressure drop of anode flow field, and elimination of bad cell module before it is used in the stack.

The assembled 5-cell compliant feed tube stack is shown in Figure 41. The cell active area of the 5-cell stack is 142 cm^2. In order to mimic the hybrid SOFC operation conditions, two preheaters that compose of a serpentine design of ¼" tubing were used to heat the air and fuel to the SOFC operating temperature. Both air and fuel preheaters were sized based on their maximum flow rates, the air and fuel could be heated up to 750°C at the stack inlets. An Isometric view of air preheater design is shown in Figure 42.

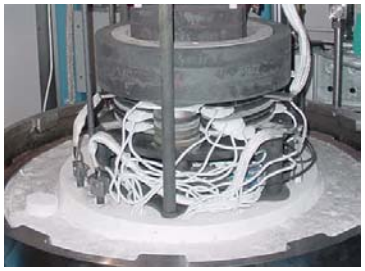

Figure 41 Assembled 5-cell compliant feed tube stack with 142 cm^2 active area per cell

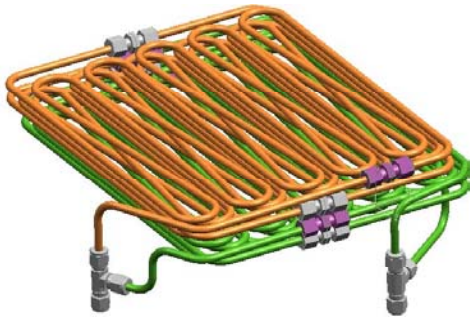

Figure 42 Isometric view of the air preheater design

3.2.2 DH06 Test Results

The 5-cell stack was heated up to 900 ◦C for curing the manifold and cathode cell seals (anode cell seal was already formed during the preseal/reduction process). Then, the stack was cooled down to 800 ◦C for normal SOFC operations. The test sequence for the 5-cell stack is listed in Table 12.

Table 12 5-Cell Stack Test Sequence

- Initial polarization curve at fixed flows with dilute hydrogen (64% H_2/balanced with N_2) (at 14.7 psia. and 800°C);
- Hold for 20 hours under constant current for conditioning (at 14.7 psia. and 800°C);
- Polarization curve at fixed flows with dilute hydrogen (at 14.7 psia. and 800°C);
- Polarization curves at fixed fuel utilization with dilute hydrogen (at 14.7 psia. and 800°C);
- Polarization curves at fixed fuel utilization with simulated SR fuel (at 14.7 psia. and 800°C);
- Polarization curve at fixed flows with dilute hydrogen (at pressurized condition and 800°C);
- Polarization curves at fixed fuel utilization with dilute hydrogen (at pressurized condition and 800°C);
- Polarization curves at fixed fuel utilization with simulated SR fuel (at pressurized condition and 800°C);
- Polarization curves at fixed fuel utilization with dilute hydrogen (at pressurized condition and different temperature);

a. Effects of fuel composition (64% H_2 vs. simulated SR fuel steam)

5-cell compliant feed tube stack, DH-06 has been tested with 64% H2 fuel and SR fuel stream, respectively. The initial performance of individual cells in the 5-cell stack, DH-06 at 800 °C and 14.7 psia are shown in Figure 43. As shown in Figure 43, cell #3 is relatively under-performing compared to other cells in the stack and the current density employed for testing of the 5-cell stack, DH-06 was limited in most cases by the low cell voltage of cell #3 (generally, current densities are adjusted to maintain all cell voltages above 0.55 V).

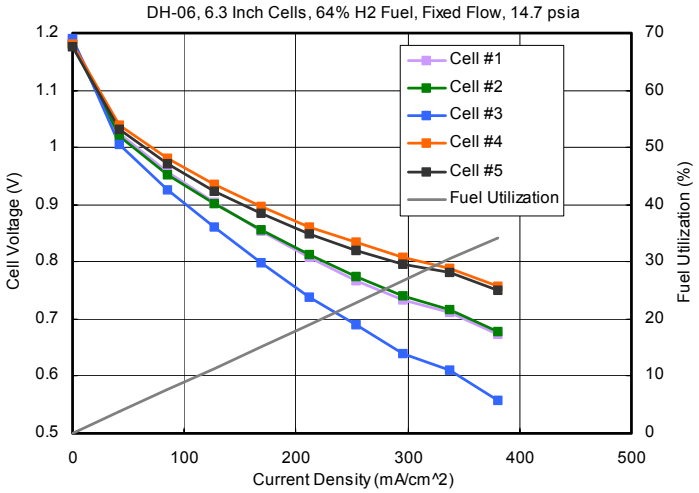

Figure 43 Performances of Individual Cells in the Compliant Feed Tube Stack, DH-06 with Diluted H_2 at 800°C and 14.7 psia

The average performance of cells in 5-cell stack, DH-06 running on 64% H_2 fuel stream under fixed flow condition was compared with that on SR fuel stream in Figure 44. Compared to 64% H_2 fuel stream, average cell voltages measured on SR fuel stream are lower by more than 50 mVs at stack operation pressures up to 61.5 psia.

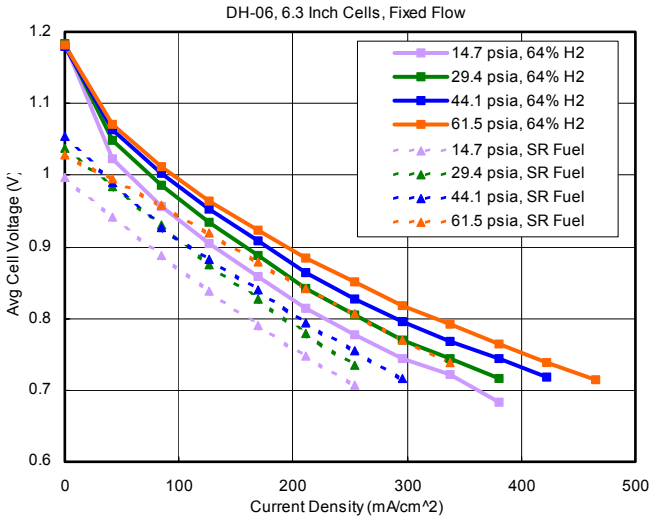

Figure 44 Performances of Average Cell in the Compliant Feed Tube Stack, DH-06 as a Function of Operation Pressure with Diluted H_2 and SR Fuel, Fixed Flow at 800°C

b. Effects of fuel utilization

The I-V curves of average cell of 5-cell stack, DH-06 at 60% fuel utilization are shown in Figure 45 and they are compared with those obtained with fixed fuel flow condition. As anticipated, cell voltages with 64% H_2 fuel stream at 60% fuel utilization appear to approach those under fixed flow condition with the increase in current density. With SR fuel stream, cell performance data at 60% fuel utilization could only be obtained at 61.5 psia due to the under-performing cell #3.

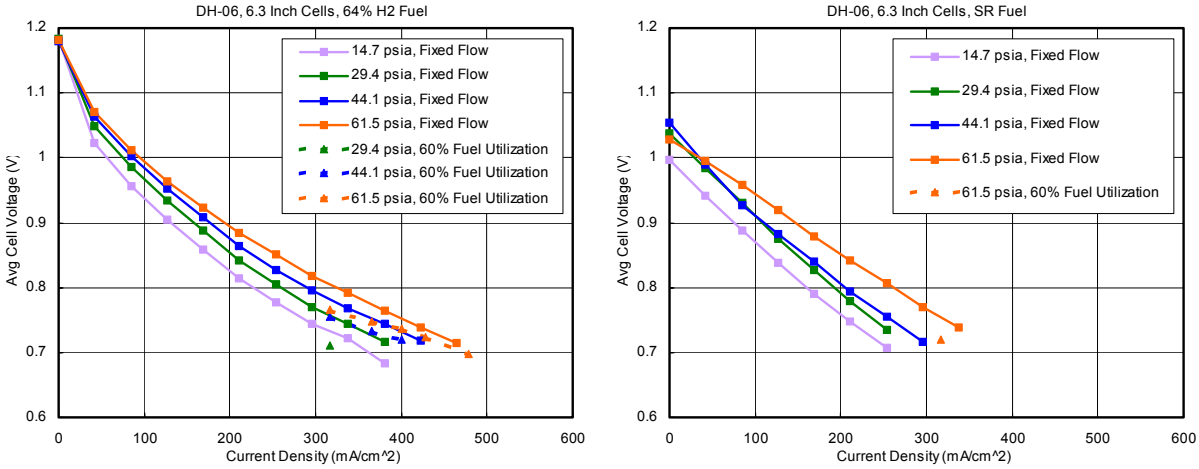

Figure 45 Performances of Average Cell in the Compliant Feed Tube Stack, DH-06 as a Function of Operation Pressure with Diluted H_2 and SR Fuel at 800°C, Fixed Flow vs 60% Fuel Utilization

c. Effects of the transition of stack operation pressure

Compliant feed tube stack, DH-06 did go through 2 pressure cycles and further testing at pressurized condition could not be made because of the abnormal rising of the temperature (up to 900 °C) in fuel exhaust manifold during the stack pressurization. The temperature rise was also accompanied by gradual drop in OCV (open circuit voltage) of cell #5 during pressurization (by as much as 80 mV). Upon depressurization, the fuel exhaust manifold returned to normal temperature, but the OCV of cell #5 remained low (lower than previous OCV by 20 mV).

Chronological analysis of observations and events showed that the initiation of cell #5 OCV drop preceded the rise in fuel exhaust manifold temperature and stack pressurization. The cell #5 OCV drop coincided with the transition of stack pressurization, i.e. fuel stream from “by-pass of back pressure regulator” to “through backpressure regulator”. The fuel exhaust manifold temperature was found to rise approximately 10 minutes after the stack pressurization started. Figure 46 shows the excursion of individual cell OCVs and temperature measurements of the 5-cell stack, DH-06.

Post-mortem test was performed after 5-cell stack, DH-06 test to find the root causes of the abnormal rising of the fuel exhaust temperature and low OCV of cell #5 and evidences that may lower the cell performance (cell #3). Crack and burning marks were found near the edge of cell #5 between the flow field and seal area (see Error! Reference source not found.). The post-mortem test also indicates that the cathode bonding is week, there is no bonding strength between cathode and cathode interconnect, especially of cell #3. A root cause analysis was performed to identify causes of the cell crack that resulted in anode exhaust temperature increase and OCV of cell #5 decrease during the stack pressure transition. Based on information gathered so far, it was suggested that the transition of fuel stream from "by-pass of back pressure regulator" to "through backpressure regulator" generated certain level of differential pressure between anode and cathode, and led to crack the cell #5. The differential pressure recorded during fuel stream transition is lower than 1 psia, but it is highly probable that local differential pressure at very short period of time during fuel stream transition may be much higher than the recorded differential pressure. The crack in cell #5 is considered responsible for the OCV drop and might have led to abnormal temperature rise in fuel exhaust manifold through accelerated crossover of fuel and air upon pressurization.

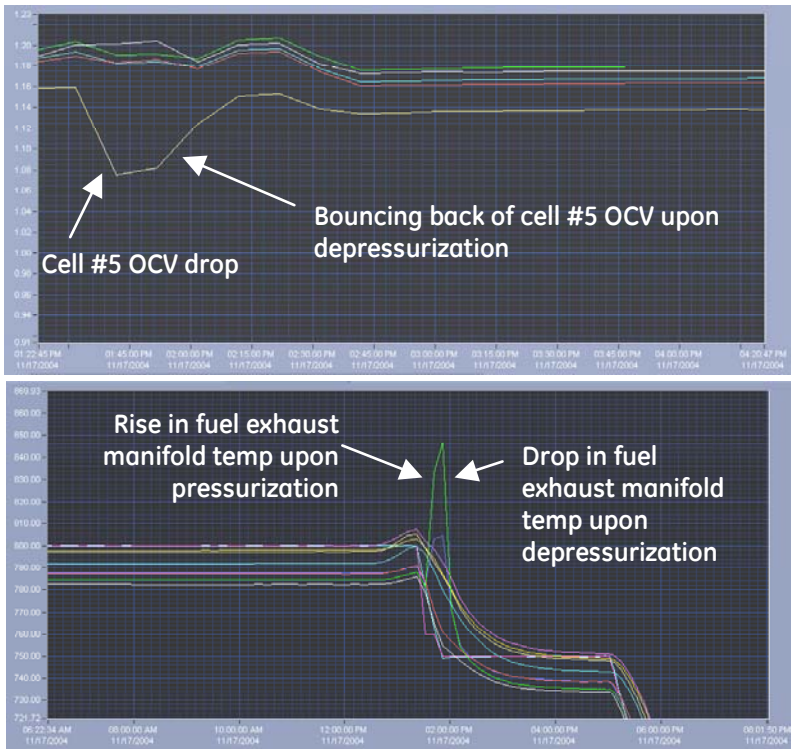

Figure 46 Observation of OCV of Cell #5 in the Compliant Feed Tube Stack, DH-06 and Fuel Exhaust Manifold Temperature during the Transition of Stack Operation Pressure

Recommended actions to mitigate the risks of cracking cell during the stack operation were identified during the root cause analysis. Since one of the potential causes for the cell crack during the operation pressure transition is the unbalanced anode and cathode seal that is introduced by cell preseal/reduction process, a one-step stack assembly process was suggested to confirm the hypothesis.

3.3 DH07: 5-Cell Compliant Feed Tube Stack Test

3.3.1 DH07 Test Setup

To confirm the hypothesis that cell crack is induced by unbalanced anode and cathode seal, a 5-cell stack, DH-07 was assembled by using compliant feed tube interconnect and following the one-step stack assembly process, i.e. omit the preseal/reduction process and assemble the stack in one step and curing the anode and cathode seal and manifold seals all together. The assembled 5-cell compliant feed tube stack is similar to 5-cell stack, DH-06 shown in Figure 41. The cell active area of the 5-cell stack is 142 cm^2. Preheaters that compose of a serpentine design of ¼" tubing were also used to heat the air and fuel to the SOFC operating temperature.

3.3.1.1 DH07 Test Results

The 5-cell stack was heated up to 900 ◦C for curing the manifold, anode and cathode cell seals. Then, the stack was cooled down to 800 ◦C for normal SOFC operations. The anode reduction was started during the stack heating up when stack temperature reached 600 ◦C. The test sequence for the 5-cell stack is listed in Table 12.

a. Effects of fuel composition (64% H_2 vs. simulated SR fuel steam)

DH-07 5-cell stack has been tested without going through fuel flow transition to avoid cell cracking problem, which has experienced in DH-06 stack test. Testing of DH-07 stack revealed that the upper 3 cells had consistently low OCVs and pressurization led to increased OCVs with the upper 3 cells. The performances of individual cells in the stack, DH-07 with 64% H_2 and fixed fuel rate at 800 C are shown in Figure 47. As shown in Figure 47, the ASR (area specific resistance) of these 3 cells was comparable or better than the other 2 cells (which showed normal OCVs). It was suggested that shorting either across the cell originating from defective cells or through manifold seal might have occurred. Post-analysis of the DH-07 stack is planned for clear explanation of the shorting problem.

The performance of cell #1 and cell #2 in the 5-cell stack, DH-07 running on 64% H2 fuel and SR fuel stream are shown in Figure 47, respectively. The fuel flow rate was fixed throughout the whole current density range. The voltage gain of 64% H_2 fuel stream over SR fuel stream is measured to be approximately 100 mV and that voltage gain translates to power density gain in the range of 15% - 18% at current density of 300 mA/cm^2.

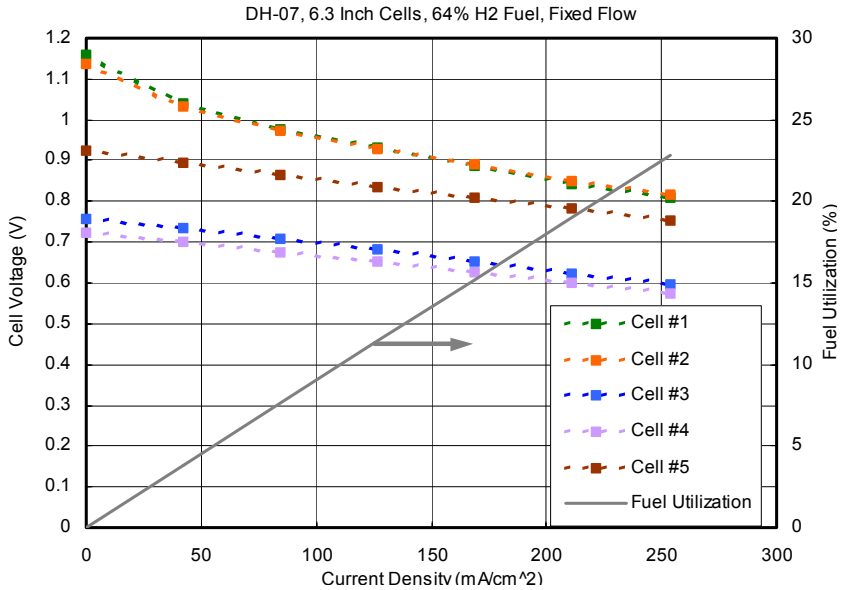

Figure 47 Performances of Individual Cells in the Compliant Feed Tube Stack, DH-07 with Diluted H_2 at 800°C and 14.7 psia

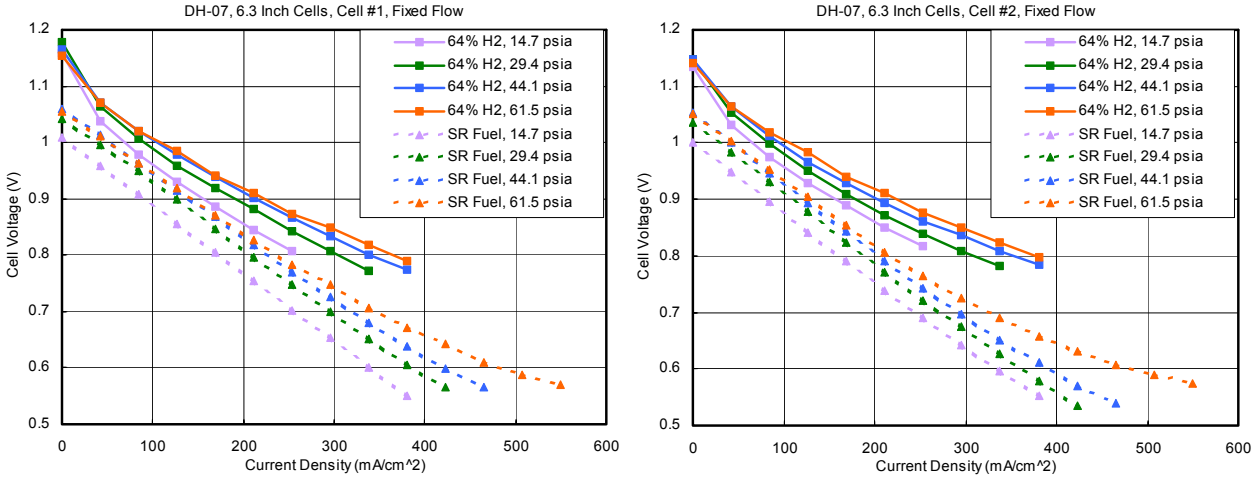

Figure 48 Performances of Cell #1 and #2 in Compliant Feed Tube Stack, DH-07 as a Function of Operation Pressure with Diluted H_2 and SR Fuel Stream, Fixed Flow at 800°C

b. Effects of fuel utilization

The performance of cell #1 and cell #2 in the 5-cell stack, DH-07 with 60 % fuel utilization is shown in Figure 48. It appears that pressurization brings I-V curves of fixed fuel utilization (60% fuel utilization in Figure 49) closer to that of fixed flow condition. Pressurization is understood to reduce mass transfer over-potential in

current generation. Therefore, cell voltage gain attained through low fuel utilization (compared to high fuel utilization) would be much less pronounced at high pressurization level.

One thing to note is that under pressurized (61.5 psia) condition, cell performance of the 5-cell stack, DH-07 was not stable at 60% fuel utilization. The cell voltage under load at 60% fuel utilization was highly noisy, unstable and continued to drop at 61.5 psia stack operation pressure. At this stage, the reason for the voltage dropping and fluctuations is not clearly understood. One possible explanation is that there might be serious leak through fuel or air manifold upon pressurization, which leads to measurable effect on cell voltage under load.

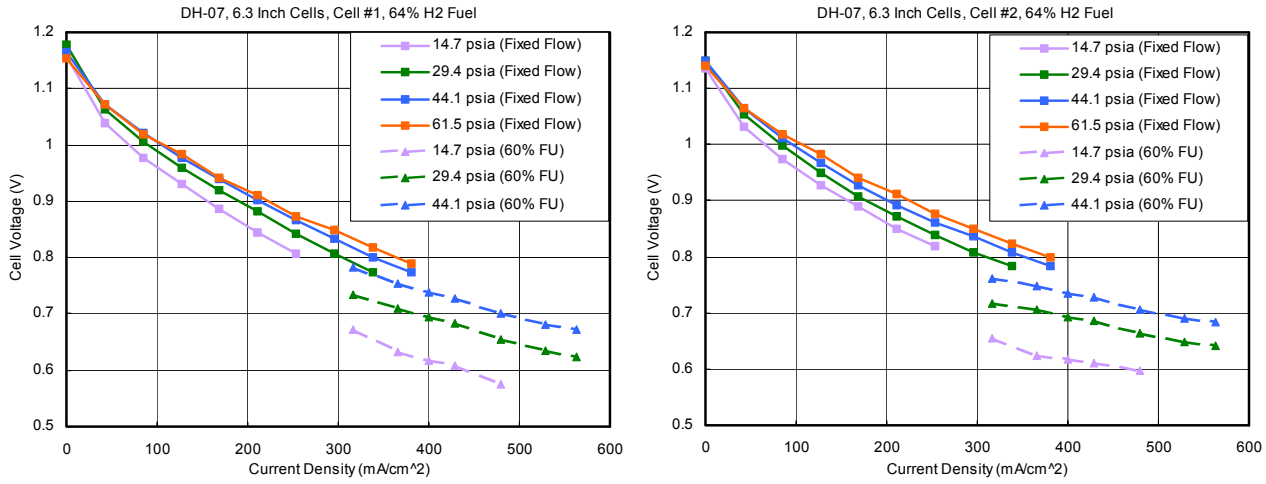

Figure 49 Performances of Cell #1 and #2 in Compliant Feed Tube Stack, DH-07 as a Function of Operation Pressure with Diluted H_2 and SR Fuel Stream at 800°C, Fixed Flow vs 60% Fuel Utilization

Conclusion

The following activities have been carried out during this reporting period. The results from these activities are summarized in this report.

- System analysis to evaluate the performance and cost impact of advanced technologies on Integrated Gasification Fuel Cell (IGFC) systems.
- Theoretical and experimental work to understand the key fabrication parameters for the fabrication of large planar SOFC cells using tape calendaring process and demonstrate the fabrication scalability to cell sizes greater than 10-inches diameter.
- Experimental work to demonstrate the operation of planar SOFC stacks of various sizes and establish the operational characteristics of these stacks under hybrid conditions.
- System analysis to establish the scale-up strategies for large (greater than 20 MW) SOFC-gas turbine hybrid systems for centralized power generation applications

References

1. Balan, et al, “Coal Integrated Fuel Cell System Study – Final Report,” January 2004, prepared by GE-Energy for the Department of Energy under DOE/NETL Cooperative Agreement DE-FC26-01NT40779
2. Balan, C., Minh, N., Rahman, F. & Andrews, R., “Coal Based SOFC System Study Baseline Concept Down Selection,” January 14, 2004, Morgantown, WV
3. “Evaluation of 450-MWe BGL GCC Power Plants Fueled With Pittsburgh No. 8 Coal,” November 1992, EPRI TR-100376, prepared by Bechtel Group, Inc., British Gas plc and Lurgi Gmbh
4. Armstrong, P., Stein, V., Bennett, D., and Foster, E. (Air Products and Chemicals, Inc.), “Ceramic Membrane Development for Oxygen Supply to Gasification Applications Ceramic Membrane,” Gasification Technologies 2002, October 2002
5. Stein, V., (Air Products and Chemicals, Inc.), Juwono, E. (ChevronTexaco Worldwide Power and Gasification), and Demetri, E. (Concepts NREC), “The Impact of ITM Oxygen on Economics for Coal-based IGCC,” 27th International Technical Conference on Coal Utilization & Fuel Systems, March 2002
6. Allam, R., Foster, E., and Stein, V. (Air Products and Chemicals, Inc.), “Improving Gasification Economics through ITM Oxygen Integration,” (IChemE) European Gasification Conference, April 2002

7. Dyer, P., Richards, and Russek, S. (Air Products and Chemicals, Inc.) and Taylor, D. (Ceramatec Inc.), “Ion Transport Membrane Technology for Oxygen Separation and Syngas Production,” Solid State Ionics 134 (2000) 21-33

8. Armstrong, P., (Air Products and Chemicals, Inc.), “Method for Predicting Performance of an Ion Transport Membrane Unit-Operation”

9. Telephone conversations, GE and Air Products and Chemicals, Inc. personnel, June 2004

10. Gangwal, S., Turk, B., Portzer, J., Gupta, R., Toy, L. (Research Triangle Institute) and Steele, R. Kamarthi, R., and Leininger, T., (ChevronTexaco), “Development of a Gas Cleanup Process for ChevronTexaco Quench Gasifier Syngas,” Twentieth Annual International Pittsburgh Coal Conference

11. Gangwal, S., Turk, B., Coker, D., Howe, G., Gupta, R., (Research Triangle Institute) and Kamarthi, R., Leininger, T. (ChevronTexaco), and Jain, S. (National Energy Technology Laboratory, WV), “Warm-Gas Desulfurization Process for ChevronTexaco Quench Gasifier Syngas,” Twenty-First Annual International Pittsburgh Coal Conference

12. Silverman, M., Henningsen, G., Ramamurthy, P., (Kellogg Brown and Root, Inc.), Gangwal, S., and Turk, B. (Research Triangle Institute), “Novel Syngas Desulfurization Process,” Twentieth Annual International Pittsburgh Coal Conference

13. Evaluation of 450-MWe BGL GCC Power Plants Fueled With Pittsburgh No. 8 Coal,” November 1992, EPRI TR-100376, prepared by Bechtel Group, Inc., British Gas plc and Lurgi Gmbh.

14. Sheldon, W. and Lyons, J., “Texaco Gasifier IGCC Base Cases, PED-IGCC-98-001,” June 2000 (Hot Gas Cleanup Case)

15. *Gasification Plant Performance and Cost Optimization,* report prepared by Bechtel Corp., Global Energy Inc. and Nexant for DOE, contract (Contract No. DE-AC26-99FT40342), May 1992 (Appendix I, subtask 1.8)

16. Telephone conversations, GE and RTI personnel, June 2004

17. Lobachyov, K., and Richter, H., “High-efficiency Coal-Fired Power-Plant of the Future,” Energy Conversion Management, Vo. 38, 1997

18. Samuelson, G.S., Rao, A. (UC Irvine), Robson, R. (Kraftworks) and Washom, B. (Spencer Management Systems, 'Vision 21 System Analysis Methodologies - 1st Semi-Annual Report, 2004. Oct. 19, 2004.

19. Rizeq, G., West, J., Frydman, A., Subia, R. Zamansky, V. (GE Global Research) and Das, K. (DOE), “Advanced Gasification-Combustion Technology for Production of Hydrogen, Power and Sequestration-Ready CO_2,” Gasification Technologies 2003, San Francisco.

20. Young, R. (Stearns-Rogers Engineering Corp.), “Recent Developments in High Pressure Entrained Flow Slagging Gasification of Coal – Update of BI-GAS Pilot Plant Operations,” Proceedings - Annual International Conference on Coal Gasification, Liquefaction and Conversion to Electricity, 1982.
21. Sokolov, P. et al, “Solid Oxide Fuel Cell Hybrid System for Distributed Power Generation - SOFC Scaleup for Hybrid and Fuel Cell Systems Final Topical Report - April 2004 to September 2004” report prepared by GE-Energy for the Department of Energy under DOE/NETL Cooperative Agreement DE-FC26-01NT40779, October 2004
22. Yegulalp, T., Lackner, K., and Ziock, H., “A Review of Emerging Technologies for Sustainable use of Coal for Power Generation,” International Journal of Surface Mining, Reclamation and Environment, 2001, vol. 15, No. 1
23. Telecon, GE-E personnel and Columbia U. personnel, 1/7/2005

Appendix 1

Table 13 Coal Composition

Coal Characterisitcs	
Coal	Pittsburgh No. 8
Coal Rank	High volatile A bituminous
Mine	Blacksville No. 1
Proximate analysis (as received), wt%	
Volatile matter	36.5
Fixed carbon	46.0
Ash	11.5
Moisture	6.0
Total	100.0
Ultimate analysis (dry), w%	
Carbon	73.2
Hydrogen	4.9
Nitrogen	1.4
Oxygen	4.9
Sulfur	3.3
Ash	12.2
Chlorine	0.1
Total	100.0
Hardgrove grindability	57
Higher heating value (as received), Btu/lb	12350
Lower heating value (as received), Btu/lb	11851
Free swelling index	7.5
Size consist as received, wt%	
Between 2" and 1/4"	45
Less than 1/4"	55
Ash Fusion temperatures, reducing/oxidizing, deg F	
Initial deformation	2018/2319
Softening	2107/2340
Hemisphere	2179/2426
Fluid	2261/2518

Table 14 Coal Ash Composition

Coal Ash Composition and Sulfur Forms	
Major ash constituents, wt%	
SiO2	45.05
Al2O3	18.45
TiO2	0.80
Fe2O3	20.31
MgO	0.98
CaO	6.09
Na2O	0.98 (soluble 0.22)
K2O	1.55 (soluble 0.003)
P2O5	0.42
SO3	5.25
Undetermined	0.12
TOTAL ASH	100.00
Coal sulfur forms, wt%	
Sulfate	0.06
Organic	1.60
Inorganic	1.64
TOTAL SULFUR	3.30

Table 15 Limestone Composition

Limestone Composition, wt%	
CaCO3	90.52
MgCO3	2.68
SiO2	5.08
Inert	1.72
TOTAL	100.00

Table 16 Bitumen Composition

Bitumen Composition, wt%	
Carbon	85.00
Hydrogen	9.70
Nitrogen	1.20
Oxygen	0.70
Sulfur	3.40
Chlorine	0.00
TOTAL	100.00